ESTIMATION OF POWER PEAKING FACTOR AND THERMAL LIMITATION ON CORE PERFORMANCE OF NIGERIA RESEARCH REACTOR-1 (NIRR-1)

BY

ANAS MUHAMMAD SALISU
M.sc./Sci/1209/2011-2012

A THESIS SUBMMITTED TO POSTGRADUATE SCHOOL AHMADU BELLO UNIVERSITY ZARIA NIGERIA

IN PARTIAL FULLFILMENT OF THE REQUIRMENTS FOR THE AWARD OF MASTER OF SCIENCE DEGREE IN NUCLEAR PHYSICS OF THE DEPARTMENT OF ;PHYSICS FACULTY OF SCIENCE, AHMADU BELLO UNIVERSITY , ZARIA NIGERIA

January, 2015

CERTIFICATION

This thesis entitle ‘Estimation of Power Peaking Factor and Thermal Limitation on Core Performance of Nigerian Research Reactor-1 (NIRR-1)’ by ANAS MUHAMMAD SALISU (M.Sc./Scin./1209/2011-2012) meet the requirement governing the award of the degree of Master of Science (M.Sc.) in Nuclear Physics and approved for its contribution to knowledge and literary appreciation.

Chairman Supervisory Committee _____ _____
Dr. Yusuf A. Ahmed. (Signature) Date

Member Supervisory Committee _____ _____
Dr. Nasiru. Rabi’u. (Signature) Date

Head of Department _____ _____
Dr. U. Sadiq. (Signature) Date

Dean Post graduation _____ _____
Prof. A. Z. Hassan (Signature) Date

DECLERATION

I ANAS MUHAMMAD SALISU (M.Sc./Sci/1209/2011-2012) hereby declare that this thesis entitle 'Estimation of Power Peaking Factor and Thermal Limitation on Core Performance of Nigerian Research Reactor (NIRR-1)' has been carried out under the Supervisions of Dr. Yusuf A. Ahmed and Dr. Nasiru Rabi'u and it has not been presented for any award of degree in any institution. All source of information are specifically acknowledged by means of reference.

ANAS MUHAMMAD SALISU (Signature) Date
(M.Sc./Sci/1209/2011-2012)

DEDICATION

This project is dedicated to my, Mother, Brothers, and Sisters and to the memory of my late Father. May ALLAH forgive and reward them with AL-JANNATIL FIRDAUS.

ACKNOWLEDGEMENT

My sincere thanks and appreciation goes to each and every individual that contributed physically, morally, financially and otherwise in making my Degree Programme a complete success.

My immense appreciation to my Chairman supervisory committee Dr. Yusuf A. Ahmed who supported and promoted this research. He generously gave me access to his book and his international journals. May Almighty ALLAH abundantly reward him and bless Him with Al-jannah and bless his family. Ameen.

My profound gratitude to my member supervisory committee Dr. Nasiru Rabi'u who motivated and corrected me on this research work. May the Almighty ALLAH bless Him and his family with Al-jannah Firdausi. Ameen

My special appreciation goes to Muhammad A. Adam of National Research Institute of Chemical and Technology (NARICT) who contributed immensely to the completion of the research. May Almighty ALLAH reward him meritoriously. Amen.

My sincere gratitude goes to the Director of Division of Agricultural Collages Prof. Fatihu Muhammad Yakasai, who give me his kind and moral support. May Almighty ALLAH reward him meritoriously. Amen.

I am thankful to the Head of Department of Physics for his moral support. May Almighty ALLAH reward him meritoriously. Amen.

My sincere gratitude goes to all staff of Center for Energy Research and Training (CERT) to mention but a few (Prof. B. B. Dewu (Director), Mal. I. M. Balarabe, Engr. A. R. Abubakar, entire Reactor Group, and CERT at large), who contributed their maximum effort in making my M.Sc. Degree Programme a complete success. May Almighty ALLAH reward them abundantly.

I am thankful to my entire family, my Mother and my late Father for the untiring support trust and investment in my life. May Almighty ALLAH forgive them and bless them with Al- jannah Firdausi.

Special thanks to my Brothers and Sisters: Ishaq, Ya'aqub, Daud, Nasir, Yusuf, Zwahruddeen, Al-yasa, Zalkifl, Iliyasu, Shuaib, Abdissalam, Fatima, and Suwaiba. May Almighty ALLAH reward them abundantly.

Beloved Friends and course mates: Aliyu Babajo, Ibrahim Usman, Aminu Isah, Buhari, Husaini Salisu, Bala Balarabe, Shamsuddeen Abdullahi, mentioned but few.May Almighty ALLAH them tankarantly.

Finally "My LORD bestows on my parent the mercy as they cherished me in childhood" amen.

ABSTRACT

The Power Peaking Factor of a reactor is known to be the ratio of its peak heat flux to the average heat flux around its core. This parameter was reported to be the key value that dictates the maximum allowable power density of a fuel assembly. Investigation shows that reactor core performance largely depends on the power peaking factor. It was in recognition of the role of this importance parameter that measurements were performed to estimate the Power Peaking Factor and core performance of the Nigeria Research Reactor–1 (NIRR-1) core, which is Miniature Neutron Source Reactor (MNSR). Our results show that the Power Peaking Factor for a preset neutron flux of 5.0×10^{11} $cm^{-2}s^{-1}$ ranges from 0.707 ± 0.293 to 1.014 ± 0.014 which yielded an average value of the estimated power peaking factor to be lower than the expected value of 1.2 with more than 20%. The thermal limitation of NIRR-1 core was also obtained which have an average of 12.6˚C. This is an in-build feature of NIRR-1 that compensates for high negative temperature coefficient of reactivity in order to keep the reactor stable at its preset power level. This is in agreement with safety requirements of the MNSR which does not permit power excursion and occurrence of boiling. However, our results show that the reactor stability is not applicable during startup and shutdown conditions. It means that utilization of the Reactor must wait some few minutes after startup to achieve stability and must stop some few minute before the shutdown. The results also indicate the need to obtain a correction factor for samples that will stay in the reactor for cyclic or longer period of irradiation provided there will be shutdown and start-up in-between the irradiations. Our results also revealed that there is a strong dependence of the reactor power on coolant temperature and rod position, which is in perfect agreement with the design of the MNSR and findings of many workers in the area. The computer program developed in this work for the determination of power peaking factor using moderator parameters will not only serve as a new source code for microcomputer control of the reactor peak power, maximum power factor and flux distribution but will also make it possible for the microcomputer console to display real time peak power level, maximum power factor thermal limitation of the reactor core, a tool that is lacking in MNSR design.

TABLE OF CONTENT

Title page	i
Certification	ii
Declaration	iii
Dedication	iv
Acknowledgement	v
Abstract	vii
Table of Content	viii
List of figure	ix
List of Tables	xi
Abbreviation	xii

CHAPTER ONE

1.1	Introduction/Background of the Study	1
1.2	Research Objectives	3
1.3	Statement of Problem	3
1.4	Justification	4
1.5	Literature review	5

CHAPTER TWO

2.0	The fission process	9
2.0.1	Reactor core arrangement	11
2.1	Leakage and Reflector on Reactor Power	16
2.1.1	Reflector Effect	16
2.1.2	Absorber Effect	17
2.1.3	Effect of Zone Refueling	17
2.2	Burn up and Control Rod Effect	19
2.3	Effect of non-fuel part of the Core	22
2.4	Flux Distribution	24
2.4.1	Distribution of Neutron Flux in the Reactor	24
2.4.2	Implication of the non-uniform Flux Distribution	27
2.5	Power Peaking Factor	29
2.5.1	Fuel Temperature Coefficient of Reactivity	30
2.5.3	Diffusion Theory Calculation	33
2.6	Heat Transfer Model	34
2.6.1	Heat Transfer Correlation Model	34
2.6.2	Heat Transfer between Fuel Cladding, Coolant and Moderator	38

CHAPTER THREE METHODOLOGY

3.1	Development of a Computer Program.	38
3.2	Determination of:	39
3.2.1	Maximum power factor inside NIRR-1 fuel rod	41

3.2.2 Thermal limitations of NIRR-1 core 41

CHAPTER FOUR RESULTS AND DISCUSSION

4.1 Results 45

4.2 Discussion 60

CHAPTER FIVE CONCLUSION AND RECOMMENDATIONS

5.1 Conclusion 64

5.2 Recommendations 65

References 66

Appendix 71

LIST OF FIGURE

Fig 2.1 fission process

Fig. 2.2. Design of the assembled RPV with internals for the three-pass core.

Fig. 2.3. Head piece of the three-pass core fuel assembly cluster with inserted control rod spider and hold-down spring (left side) and sealing concept (right side).

Fig 2.4: Effect of reflector on neutron

Fig.2.5: Effect of absorber on neutron flux

Fig 2.6: Is the axial and radial from the center of the reactor

Fig. 2.7: Distributions of the flux along the radius

Fig: 2.8: Radial Distribution of a flux

Fig: 2.9 a variation of flux and distance

Fig: 2.10. Radial Distributions of the flux

Fig. 4.1**:** Reactor Power Peaking Factor obtained using measured coolant temperature rise for 1hr

Fig. 4.2**:** Reactor Power Peaking Factor obtained using measured coolant temperature rise for 6hrs

Fig. 4.3**:** Reactor Power Peaking Factor obtained using measured coolant temperature rise for 6hrs

Fig. 4.4**:** Reactor Power Peaking Factor obtained using measured coolant temperature rise for 6hrs

Fig. 4.5**:** Reactor Power Peaking Factor obtained using measured coolant temperature rise for 6hrs

Fig: 4.6: Reactor Power Peaking Factor obtained using measured coolant temperature rise for 6hr

Fig. 4.7 Reactor Power Peaking Factor obtained using measured control rod position for 6hrs

Fig. 4.8 Reactor Power Peaking Factor obtained using measured control rod position for 6hrs

Fig. 4.9 Reactor Power Peaking Factor obtained using measured control rod

position for 6hrs

Fig. 4.10 Reactor Power Peaking Factor obtained using measured control rod position for 6hrs

LIST OF TABLES

Table 4.1: Reactor Power Peaking Factor obtained using measured coolant temperature rise for 1hr

Table 4.2: Reactor Power Peaking Factor obtained using measured coolant temperature rise for 6hrs

Table 4.3: Reactor Power Peaking Factor obtained using measured coolant temperature rise for 6hrs

Table 4.4: Reactor Power Peaking Factor obtained using measured coolant temperature rise for 6hrs

Table 4.5: Reactor Power Peaking Factor obtained using measured coolant temperature rise for 6hrs

Table 4.6: Reactor Power Peaking Factor obtained using measured coolant temperature rise for 6hrs

Table 4.7: Reactor Power Peaking Factor obtained using different control rod position in cm

Table 4.8: Reactor Power Peaking Factor obtained using different control rod position in cm

Table 4.9: Reactor Power Peaking Factor obtained using measured control rod position for 6hrs

Table 4.10: Reactor Power Peaking Factor obtained using measured control rod position for 6hrs

ABBREVIATION

NIRR-1	Nigeria Research Reactor-1
MNSR	Miniature Neutron Source Reactor
PWR	Power Reactor
HNNA	Hopfied Neural Network Artificials
PPF	Power Peaking Factor
LSM	Linear Superposition Model
PARET	Computer Analysis Code
HEU	High Enrich Uranium
LEU	Low Enrich Uranium
WER/1000	Water Moderated Energy Reactor/1000
RPV	Reactor Pressure Vessel
CRGA	Control Rod Guide Assembly

CHAPTER ONE

(Introduction)

1.1 Introduction/Background of the Study

In a light water moderated reactor, the normal case is where an assembly consists of only one kind of fuel rod of U^{235} enrichment, the corner fuel rod nearest to the cruciform water- gap generates the highest power in the assembly. The ratio between the highest power and that average over the assembly is called the Power Peaking Factor (PPF), and is a key value that dictates the maximum allowable power density of the assembly. (In Ho Bae *et al.,* 2009, Vladimir *et al.* (2011) and Yashar *et al*., 2012)

An important problem in the design of the fuel assembly is how to depress the Power Peaking Factor. A commonly adopted expedient to flatten the power distribution is to use fuel rods that are allowed in enrichment at the corners. Limitation are imposed on this expedient by local power peaking produced at different position in the fuel assembly by excessive lowering of the enrichment at the corners, and by the impairment that would expected of the multiplication factor with the use of too many fuel rod with low enrichment. This calls for optimization of the enrichment distribution within individual fuel assemblies. (Vladimir,*et al*. 2011).

The Nigeria Research Reactor-1 (NIRR-1) is a 31kW of power tank-in-pool Miniature Neutron Source Reactor (MNSR). It has ten irradiation channel, one control console, two rabbit systems and computer control system of these ten only six are connected to the rabbit systems. The small core of the reactor is cooled and moderated by light water, while annular beryllium surrounding the core acts as reflector. The MNSR designer's objectives were to achieve a core of low critical mass, with a small compact structure. Under moderation was achieved by choosing highly enriched uranium (U-235) of 90.2% as fuel material and light water as moderator. Materials with

low neutron captures cross section and are desirable in moderation of processes reactor. (Ahmed, *et al*., 2013).

The safety of the MNSR is augmented by the 197 ratio of hydrogen to uranium-235, which enlarges the degree of under moderation of the core, increase the negative temperature of reactivity and enhance the temperature feedback. Also the ratio of the core height to diameter was optimized to 1.0 to take care of the axial neutron flux fraction, to boost the coupling of the outlet and inlet flow, to show then the time of temperature feedback and increase the worth of the top beryllium reflector used for the extension of life time of the core. (Zhu, 1990, Guo, 1983,)The removal of the heat from the core is achieved by water recirculation and natural convection (Guo, 1983; Shi, 1990). The thermal hydraulics simulation tests safety experiment shows that for the thermal hydraulic to yield the desired rise in temperature, the height inlet orifice for MNSR must remain at 6mm and that of the outlet orifice at 7mm.(Ahmed *et al*. 2008).The NIRR-1 MNSR is operating at Negative Temperature Coefficient which varies inversely with the reactivity of the Reactor. Fuel power density must be limited due to temperature, thermal hydraulic and mechanical design limitations. In NIRR-1 temperature limitation is imposed by internal hydrogen pressure due to temperature dissociation. (Ahmed *et al*. 2008). These design consideration will be utilize in this study to investigate NIRR-1 Power Peaking Factor and Thermal Limitations on Core Performance.

1.2 Aim and Objectives

The aim of the thesis is to estimate the Power Peaking Factor and Thermal Limitation on Core Performance of NIRR-1. Our objectives are therefore:

1 To use NIRR-1 parameters to develop computer program.

2 To use the program developed and NIRR-1 coolant temperature values to determine:

a. Maximum Power Factor inside NIRR-1 core

b. Thermal limitations of NIRR-1 core

3 To evaluate of the dependency of maximum power on temperature

1.3 Statement of Problems

In a nuclear reactor, the neutron in the core of the reactor determines the dynamic behavior of the reactor. In order for the power generated by fission reactions to be maintained at a constant level, the fission rate most remains steady over the course of time. In water cooled reactor like NIRR-1 (MNSR), the predominantly reactivity changes are brought about by change in the moderator (coolant temperature) and power which cause in decrease in reactivity. This property is called Temperature Coefficient of Reactivity. It therefore became important to monitor the power and thermal limitation (moderator coolant temperature) in any Reactor to ascertain:

(i) If a transient decrease in temperature occurs in the Reactor following an increase in the reactivity, the Negative Temperature Coefficient of Reactivity sets is to allow decrease in the rate of heat generated. In the event the reactor is having positive temperature coefficient, the reactivity increase will lead to temperature increase as well (Ahmed *et al*. 2008). The investigation of the temperature coefficient became necessary.

(ii) The flux density determines the power of the reactor and visa vi. In the event that power escalation occurs, the reactor inherent safety may not be able to withstand power and temperature increase. It is therefore imperative to ascertain maximum power of the reactor under all conditions.

A temperature coefficient of reactivity is thus a desirable feature since it is an important factor in the reactor stability and operational safety. The single control rods in the design of NIRR-1 constitute a single point failure. The rod, which is a shim rod and expected to compensate for small reactivity transient caused by change in load demand, core temperature and power level maneuvering, could not stand severe conditions. The control rod cannot shutdown the Reactor when it stuck in full "out" position. Since the reactivity of the reactor is linearly related with flux and power distribution, the position of the control rod in the core at any point in time need to be monitored to establish the density or relative strength of the reactor flux. (Ahmed, *et. al*., 2008).

1.4 Justification

In a nuclear fission Reactor, the neutron flux distribution in the core determines the power and dynamic behavior of the reactor. The thermal neutron flux achieves its maximum value in the center of reactor and falls to zero at the extreme ends of the Reactor core since very few thermal neutrons are produce in this area, hence the flux distribution is strongest at the middle of the reactor's core (Ahmed, *et al*. 2008). However, the average flux of a Reactor is a variable parameter that depends on the Reactor's moderator and coolant temperature. These parameters are to be monitored for every Reactor from time to time to establish the stability of the reactor's flux. It has been shown that reactor flux stability is a requirement for Neutron Activation Analysis

(a major utilization of the Reactor) and precious stone irradiation (Jonah *et al*., 2005; 2006; Kapsimalis, *et al*., 2009; Ahmed, *et al*., 2010; 2013; Njinga *et al*, 2011).

Since the commissioning of NIRR-1 in 2004, several attempts were made to measure its flux stability using Activation foils method (Musa, *et al*., 2012,), and also to ascertain its flux variation (Ahmed, *et al*., 2008), maximum operable time (Ahmed *et. al*., 2011) and effects of poisoning (Ahmed, *et al*., 2012). However, there were no efforts to determine its Power Peaking Factor as a means to establish the flux stability.

In addition, NIRR-1 has single central control rods which perform both regulatory and shim functions (Njinga, *et al. 2011*).In case of emergency such as rod stuck in fully out position, reactor shut down is achieved by pumping of cadmium rabbit and cadmium string into the inner irradiation channels. This single failure may lead to power excursion and radiation exposure of personnel hence, there is need to know the power factor and thermal limitation of core performance. That is Local Power Peaking Factor should be determined precisely to ensure that a number of safety limits imposed on the fuel pellets and fuel clad barriers are not violated during normal reactor operation.(Vladimir *et al*., 2011). The present works therefore seek to address both flux stability and single point of failure concerns mentioned above.

1.5 Literature Review

Previous work by Ahmed *et al*., 2008, Khamis and Alhalabi 2007, Hainoun and Alias 2005, demonstrated the dependence of neutron flux and power of a Miniature Neutron Source Reactor (MNSR) on thermal hydraulic parameters and that the flux values could be exploited to predict the reactor fission power and flux distribution. However, they did not extend their works to Power Peaking Factor of the MNSR and its relationship with the thermal hydraulic parameters.

Publications by Balogun, 2003, Jonah *et al*., 2007, Ahmed, *et al*., 2010, Ahmed, *et al*., 2011, Musa, *et al*., 2012, Ahmed, *et al*., 2013 attempted to review the NIRR-1 core excess reactivity due to fuel burn up and temperature effects. Their findings show that there is a strong correlation between the reactor's operating time and its coolant temperature with the core excess reactivity. They concluded that for a clean core excess reactivity of 3.77 mk, 5 and 8 h are the optimum times for the operation of Miniature Neutron Source Reactors under the two flux conditions (full and half power, respectively). These results have set boundary conditions for determination of power peaking factors, which we hope to investigate.

The Syrian group (Khamis and Alhalabi 2007) exploited the temperature effect of their MNSR to study the potential benefit of increasing cooling time on operational characteristic of the Syrian MNSR for various scheme of cooling. They showed that additional cooling of the moderator extends the operational time of the MNSR. This is in agreement with the fact that temperature and reactivity are inversely proportional. It also gave a clue to the fact that power peaking factor can be control using thermal hydraulic parameters.

Earlier on Ahmed, *et al*., 2002, studied the possibility of using k_0 – standardization method, based on HØgdahl convection to predict flux distribution in irradiation channel of NIRR-1. The authors used the concept of resonance energy and non-ideality of epithermal neutron flux distribution to examine its implication on essential nuclear data parameter relevant to k_0 formalism. The authors were able to show that reactor flux stability is a requirement for neutron activation analysis and need to be monitored from time to time.

In Ho Bae *et al.*, (2009), worked on Support Vector Machines (SVMs) to estimation of the power peaking factor in a nuclear reactor and uncertainty analysis and

concluded that knowing more about the Local Power Density (LPD) at the hottest part of a nuclear reactor core can provide more important information than knowledge of the LPD at any other position and the LPD at the hottest part needs to be estimated accurately in order to prevent the fuel rod from melting in a nuclear reactor. This paper has shown that estimation of power peaking factors, which our work hopes to achieve with NIRR-1, is very important in order to know the safety of the reactor.

Using the nuclear reactor analysis code PARET, Muhammad (2013) worked on uncontrolled reactivity insertion transients of a material test research reactor fuelled with high density U_3Si_2 dispersion fuels. He determined the reactor performance under reactivity insertion transients with totally failed control rods and the reactivity feedback during the transients. It was observed that the reactor stabilizes at new power levels which were lower than the original power, with the power of HEU fuelled reactor slightly lesser than that of the LEU fuelled reactor. He finally determined the reactor performance under loss of flow transients with totally failed external control systems. The work demonstrated the ability of the analysis code PARET to predict the transient behavior of reactors especially reactivity and power. Since our group is not in possession of such a code, we developed a simple computer program that will determine such parameters in our work.

Using Monte Carlo modeling of a PBMR-400 Vladimir, *et al*., 2011 determineindividual pebble temperature peaking factor due to local pebble arrangement in a pebble bed reactor core. In their work they concluded that the stochastic nature of the pebble bed cannot lead to highly elevated fuel temperatures but rather local or core-wide coolant flow reductions are the likely cause. This finding attracts a lot of attention on whether to determine individual or collective Power Peaking Factors of fuel elements. However, since NIRR-1 core is a sealed one with no online refueling, a

collective determination of the Power Peaking Factor is more desirable and yields more accurate values.

Recently, Musa *et al*., 2012 determined the radial and axial neutron flux distribution in irradiation channel of the NIRR-1 using foil activation technique. This attempt is to characterize the newly installed cadmium-lined irradiation channel in the reactor. There results show that the installed cadmium line did not affect NIRR-1 flux stability. As an extension of the work, we ventured here into determination of the reactor's power parameters.

More recently, Shima and Ali (2013) studied axial variation of enrichment distribution method and radial variation of enrichment distribution in VVER/1000 reactor using a Hopfield neural network to optimize fuel management. They investigated appropriate ways to solve the problem of optimizing fuel management in VVER/1000 reactor. They suggested the use of coupled programs, which one of them is the nuclear code, for making a database and modeling the core, and another one is Hopfield Neural Network Artificial (HNNA).

The present studies hope to estimate the Power Peaking Factor and thermal limitation of NIRR-1. This we hope to achieve by using a Computer program and by solving diffusion and transportation equations.

CHAPTER TWO

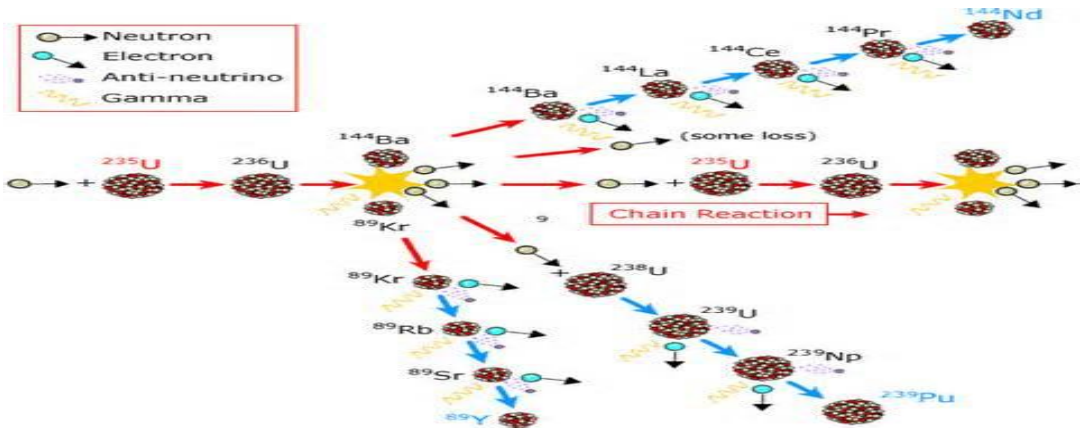
(Theoretical Considerations)

2.0 The Fission Process

When a nucleus fissions, it splits into several smaller fragments. These fragments, or fission products, are about equal to half the original mass. Two or three neutrons are also emitted. The sum of the masses of these fragments is less than the original mass. This missing mass (about 0.1 percent of the original mass) has been

converted into energy according to Einstein's equation. (Fig 2.1,) Fission can occur when a nucleus of a heavy atom captures a neutron, or it can happen spontaneously. (Nuclear fission)

An induced fission reaction. A neutron is absorbed by a uranium-235 nucleus, turning it briefly into an excited uranium-236 nucleus, with the excitation energy provided by the kinetic energy of the neutron plus the forces that bind the neutron. The uranium-236, in turn, splits into fast-moving lighter elements (fission products) and releases three free neutrons. At the same time, one or more "prompt gamma rays" (not shown) are produced, as well. In nuclear physics and nuclear chemistry, nuclear fission is either a nuclear reaction or a radioactive decay process in which the nucleus of an atom splits into smaller parts (lighter nuclei). The fission process often produces free neutrons and photons (in the form of gamma rays), and releases a very large amount of energy even by the energetic standards of radioactive decay. (Nuclear fission)



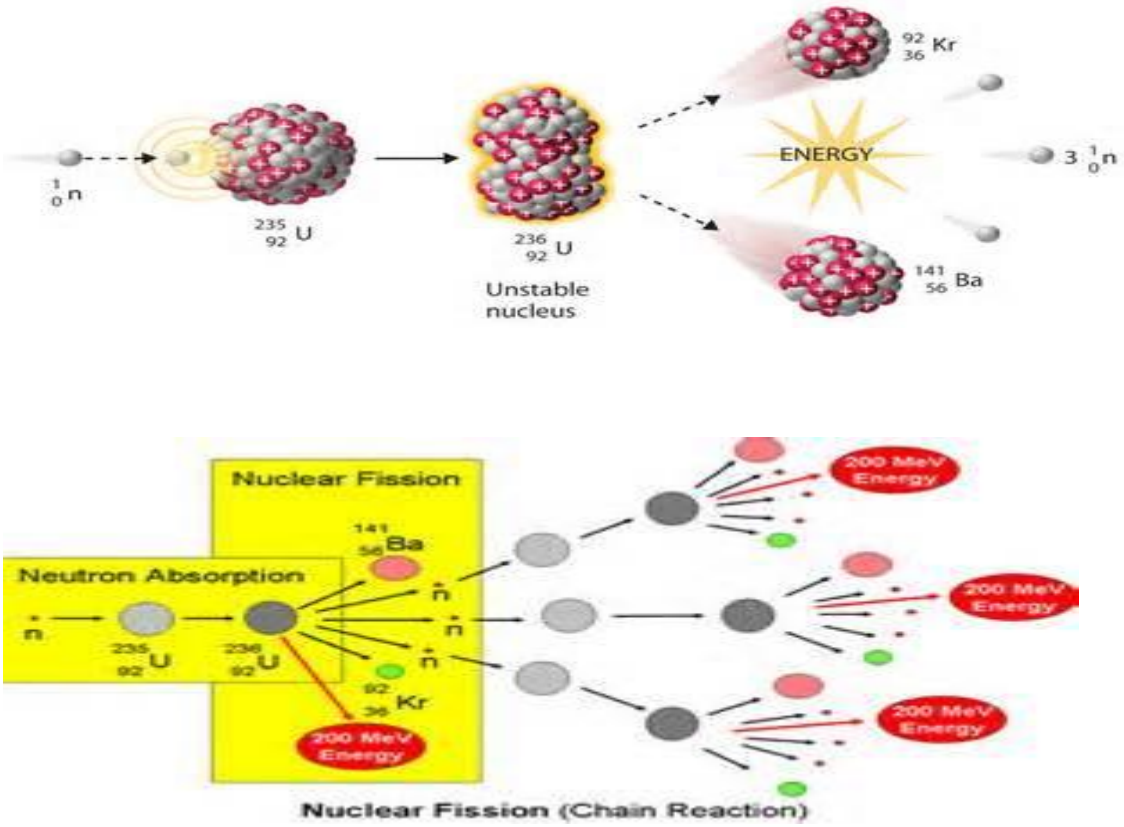


Fig 2.1 (fission process)

2.0.1 Reactor Core Arrangements

The reactor concept is based on the design and can be seen in Fig. 4, showing a segment of the reactor pressure vessel (RPV) with outlets, the core barrel, steel reflector, control rod guide assembly (CRGA) and the positioned steam plenum. For simplification, only a single fuel assembly cluster is displayed here. The core barrel is suspended at the lower vessel top and centered in radial direction using four centering elements. The alignment in vertical direction is realized using protruding supports at the bottom of the vessel. The core barrel sits, together with the control rod guide assembly, on a ledge machined from the RPV flange and is preloaded with a spring

element. The lower vessel is braced with the closure head flange using reduced shank bolts and nuts. Two O-ring seals ensure leak tightness between the closure head and the lower RPV. For the three-pass core design, the coolant has to be mixed in the mixing chambers above and below the core. The lower mixing plenum, which is welded to the bottom of the lower core plate, homogenizes the water flow from the down comer before it enters through the plate into the lower part of the evaporator. In the peripheral section of the lower mixing chamber, the coolant from super heater 1 is mixed before it enters super heater 2. The heated, supercritical steam is collected and mixed above all fuel assembly clusters in the steam plenum. The space above the steam plenum is designed to house the guide tubes for the control rods. Each guide tube is centered individually at the top of the steam plenum using the corresponding head piece bushing of the FA cluster proposed by (Fischer *et al*., 2009). The design challenges for the RPV are the thermal expansions between the core barrel, the steam plenum and the RPV. If the steam plenum would be allowed to move with the expanding core barrel during operation, the fixed hot pipes would jam inside the steam plenum and the C-ring seals would fail. Therefore, in this design, the steam plenum rests on the support brackets inside the lower vessel, while the core barrel is suspended at the closure head flange. With this concept, thermal expansions between the internals and the RPV are decoupled and thermal stresses are avoided. Another design challenge results from the high temperature difference of the hot pipes, which will have super heated steam with a temperature of 500^0C in the inside of the pipe, compared with the inlet coolant at 280^0C inlet temperature at the outside. A thermal sleeve has been designed by Fischer *et al*., (2009) to prevent contact of the hot pipes with the outlet nozzles of the RPV. The dimensioning of the RPV and closure head as well as the design calculation for the studs, nuts and O-ring seals is performed using the safety standards. The boiler

equation serves as the basis to calculate the different wall thicknesses of the cylindrical and the spherical parts of the vessel. A second stress analysis is performed for the core internals carrying heavy load. This is the case for the flange of the core barrel and the flange of the core support plate, carrying the weight of the core internals and the support brackets of the RPV, where the steam plenum is mounted.

For example, the core

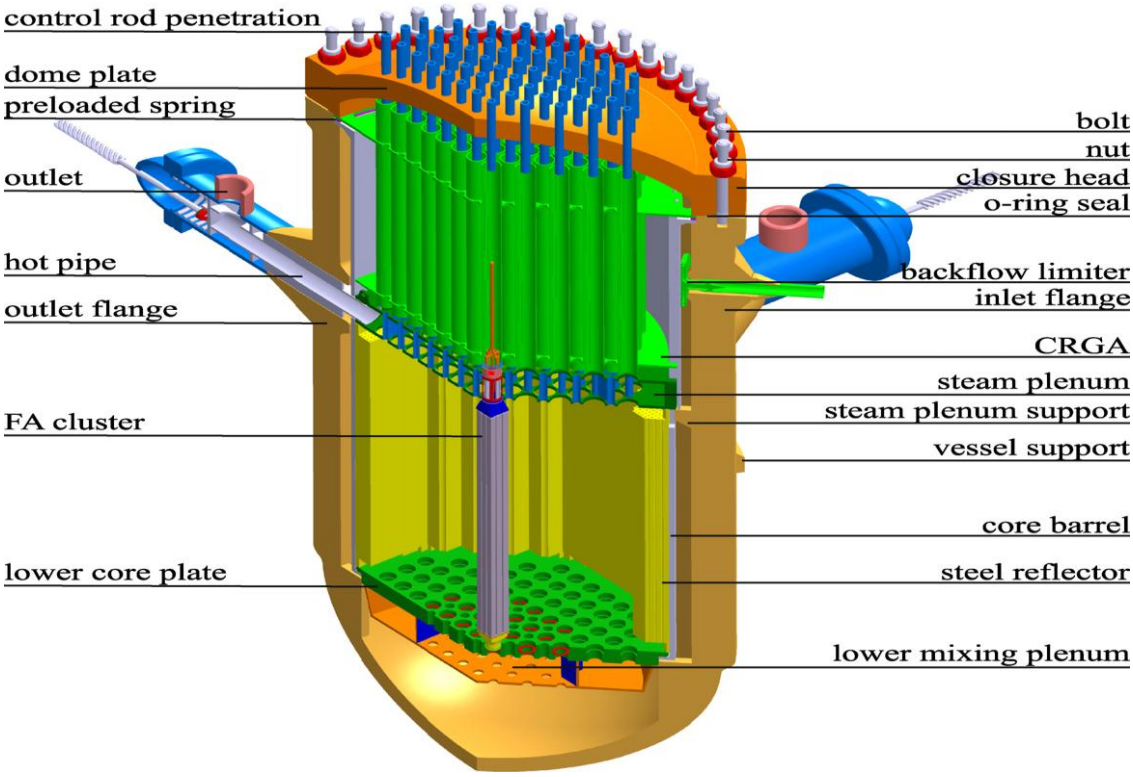


Fig. 2.2. Design of the assembled RPV with internals for the three-pass core. (Fischer et al.,2009)

The foot piece is designed with an upper plate, a lower plate and a diffuser (which becomes a nozzle in case of the first super heater), as shown in Fig. 2.2. All but the central assembly box of the cluster are welded with the upper plate. The central assembly box is bolted with four assembly box screws with the upper plate, instead. This central box is carrying the cluster weight when the cluster is lifted up. The other eight assembly boxes are sliding with their upper ends in the head piece to avoid

thermal deformations of the cluster in case of different assembly temperatures (see Fig. 2.2, right side). All central moderator boxes inside the assemblies are welded to the top of the head piece. Their lower ends are extended with cylindrical tubes which are inserted into the lower plate of the foot piece, where the moderator water is released to be mixed with the gap water surrounding the assemblies (indicated flow path with blue arrows in Fig. 2.2). These holes can be used as outlet orifices to adjust the mass flow rate through the moderator boxes. Openings for the vertical steam flow, which are surrounded by the lower plate, are designed as large as possible to minimize pressure losses. The lower plate of the foot piece and the diffuser are welded together to avoid leakage of cold moderator water into the superheated steam. The diffuser features circumferentially arranged alignments to position the cluster in the core and to prevent rotational movement. After insertion of the fuel rod bundles into the assembly boxes, the lower plate and the upper plate of the foot piece are bolted together with eight assembly cluster screws of size M8. This way, the lower plate keeps the fuel bundles in place. The upper plate and the lower plate have sealing lips at their contact surfaces, which are pressed together by the assembly cluster screws. The total arrangement is completely separating moderator and steam mass flows without any significant leakage. If necessary, a fuel rod can be replaced during revisions, e.g. for inspection, with the following disassembly steps. The cluster is turned upside down, the 12 bolts of the foot piece are opened, and the fuel rod bundle is pulled out. After opening the four bolts of the carrier plates, each row of fuel rods can further be disassembled by drilling out the bolt rivets of the dedicated rod (see Fig. 2.2, right side). The cluster is reassembled in reverse order. The head piece of the assembly cluster consists of a bottom plate with nine round openings for the cylindrical extensions of the assembly boxes, a transition nozzle between the square cluster geometry and the cylindrical openings of the steam

plenum, a cylindrical window element with large openings to release the steam, and a bushing screwed on top of the head piece to pull out the cluster. The head piece is shown in Fig. 2.3. All but the inner assembly box are sliding in the bottom plate of the head piece. Two piston rings, shown in Fig. 2.3, is avoid leakage. The central assembly box is welded together with the bottom plate. The bottom plate, the transition nozzle and the window element are welded together as well. Two metal C-rings are applied to the window element to minimize leakage of moderator water into the steam plenum, which has already been described for the one-pass core head piece by (Fischer *et al.*, 2009). The extensions of the moderator boxes, of which four are round to be bended to fit into the window element, are welded into the top plate of the window element. The other five moderator boxes have straight extensions to allow insertion of control rods from the top.

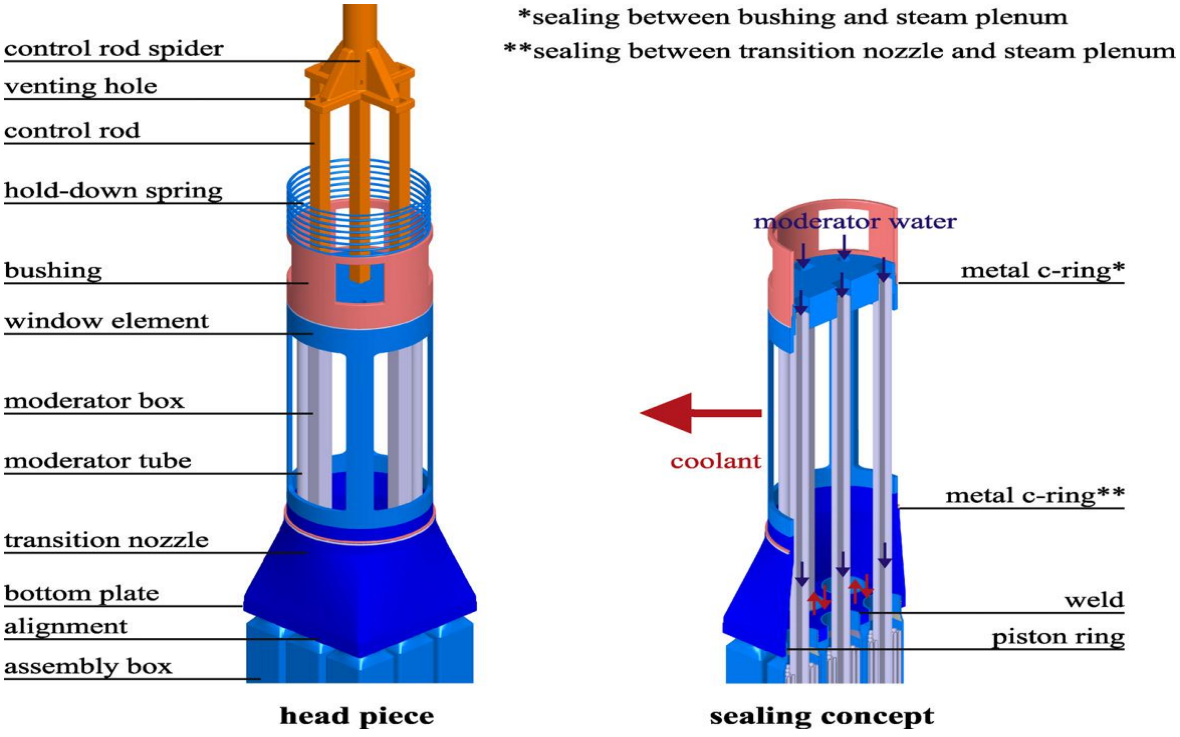


Fig. 2.3. Head piece of the three-pass core fuel assembly cluster with inserted control rod spider and hold-down spring (left side) and sealing concept (right side).

2.1 Leakage and Reflector Effects

Even if the core is homogeneous and compact the flux and power density is affected at the core reflectors boundary, typical example is given below.

2.1.1 Reflector Effect

In this case, the control rod is not inserted in the central area of the core, therefore no depression of the thermal flux and thus no flatting of flux distribution. One can then deduce that: (module 10)

a) A flatting of the thermal neutron flux in the core is achieved. That is to say that the average/maximum flux ratio is increased. As seen in Fig. 2.1, the "hump" in the flux distribution is due to the leakage of fast neutrons into the reflector, where they are thermalized. Since the reflector contain no absorber of thermal neutrons, it behaves as (is equivalent to) a source of thermal neutrons.

b) Due to the increase in the contour of the core, there is a better utilization of neutrons in the outer area of the reactor, which contributes greatly to the generated power.

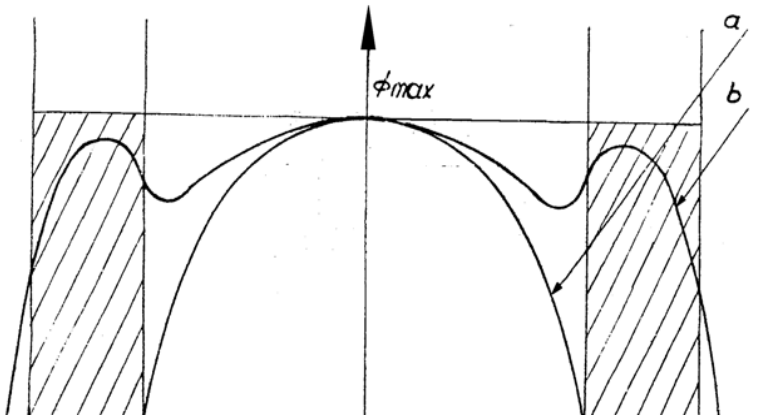


Figure 2.4: Effect of reflector on neutron (module 10)

Where: 'a' = flux without reflector,

'b' = flux with reflector

2.1.2 Absorber Effect

In this case rod (absorber) is inserted in the central area of the core, depressing the thermal flux and thus flatting flux distribution. (module 10)

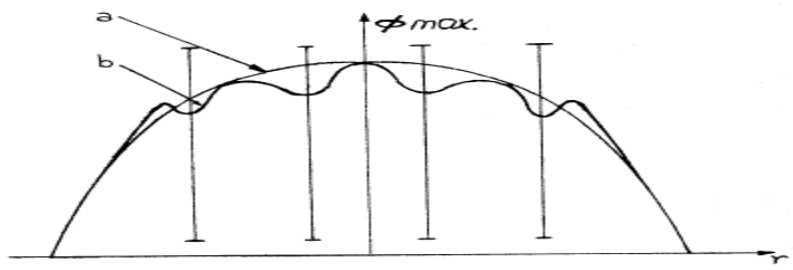


Fig.2.5: Effect of absorber on neutron flux

Where: a: flux without reflector,

b: flux with reflector.

The control rods soak up part of the excess reactivity, which is found in the core and is detrimental to the k_{eff}.

2.1.3 Effect of Zone Refueling.

Zone refueling means that fuel in the central channel is left for a longer period of than the fuel in the outer channel so as to achieve a high burn up level. Thus the central fuel elements generated relatively fewer neutrons than the outer elements. For the effect of flux flatting on a natural uranium core, the expression for the power in a natural uranium core is thus (module 10):

$$\boldsymbol{P = \frac{\emptyset . M}{3 \times 10^{12}}} \qquad (2.1)$$

where, P=: power in MW(t)

M=: mass of uranium (in ton), and

Φ=: average thermal flux, (in n $cm^{-2}s^{-1}$).

It may be observed from the formula that there are enormous economic benefits to be gained from increasing the average flux without increasing the maximum flux.

2.2 Burn Up and Control Rod Effects.

An important parameter in the design and analysis of a nuclear reactor is the reactivity worth of the control rod which is a measure of the efficiency of the control rod to absorb excess reactivity. During reactor operation, the control rod worth is affected by factors such as the fuel burn up, Xenon concentration, Samarium concentration and the position of the control rod in the core.

The reactivity worth of control rods which is their efficiency to absorb excess reactivity is an important parameter in the design and analysis of a nuclear reactor core (Khan, *et al.*, 2009). The control rods worth is affected by their position in the core, their operational time, surrounding materials, fuel burn-up as well as the concentrations of fission products such as Xenon and Samarium.

An essential requirement of the control system is that it must be capable of introducing enough negative reactivity to compensate for the built-in (positive) reactivity at initial start-up of the reactor (Khan, *et al.*, 2009).The method of Reactor control employed in MNSR's like NIRR-1 is the withdrawal or insertion of the central control rod made of cadmium. Control rod insertion leads to absorption of neutrons in its vicinity and causes a distortion of the neutron flux distribution.

The control rod worth is one of the important data for management of Reactor operation, and used for the prediction of control rod position at start-up and the estimation of the excess reactivity during the reactor operation. Because the control rod worth would be affected by fuel burn up, the difference between the measured control rod worth and the actual one would be enlarged as the fuel burns up. In particular, the control rod worth would change after the fuel exchange. For these reasons, it must be necessary to grasp the control rod worth precisely to operate the reactor more safely. Hafnium (Hf) is used as neutron absorber in JRR-3. Neutron absorption cross section of

Hf is large, and the isotopes produced by neutron absorption have similar cross sections. The ^{181}Hf becomes the ^{181}Ta by β decay in half-life of 45 days, and ^{181}Ta(n,γ)^{182}Ta has about 21barns as the thermal neutron absorption cross section. That is why ability as the neutron absorber does not change by burn-up greatly. In the equilibrium core, when follower fuel burn-up is lower than the average burn-up, the worth becomes smaller as follower fuel burn-up increases. And when follower fuel burn-up becomes higher than average burn-up, the worth does not change so much. The reason is as follows: When follower fuel burn-up is lower than average burn-up of core, it is easy to fission than other fuel. Therefore the reactivity change by the burn-up of follower fuel is large, and the influence is large. But when follower fuel burn-up is higher than average burn-up, it is hard to fission than other fuels. Therefore the reactivity change by the burn-up of follower fuel is small, and the influence to give control rod worth is very small. (Khan, *et al.*, 2009).The control rod worth was calculated as follows:

$$\Delta\rho = \frac{k_0 - 1}{k_0} - \frac{k_T - 1}{k_T} \qquad (2.2)$$

where $k_0 = k_{eff}$ with control rods completely withdrawn,

$k_T = k_{eff}$ with control rods completely inserted (IAEA TECDOC-643, 1992).

Three types of control rod materials, namely Ag–In–Cd, B_4C and Hf were used. Burn-up level for each fuel element in the core is one the most important parameters for in-core fuel management. During reactor operation the burn-up level (B) is calculated according to the following equation which actually shows the energy generation per initial heavy metal loading (W^0) in the fuel element:

$$B_m^{t+\Delta t} = B_m^t + \frac{1}{W_m^0}\int_t^{t+\Delta t} Q_m \mathrm{d}\tau \qquad (2.3)$$

Where the power generation by the *m*th fuel element (Q_m) with its volume V_m is defined as:

$$Qm \equiv \int V \in Vmq(x,y,z)\ \mathrm{dV} = \gamma \int V \in Vm\Sigma f(x,y,z)\ \Phi(x,y,z)\ \mathrm{dV} \qquad (2.4)$$

Here, γ and Σ_f denote the energy released per fission and the macroscopic fission cross section. The neutron flux distribution, $\phi(x, y, z)$, needed in the equation is obtained from the solution of the reactor eigenvalue problem of the neutron diffusion equation:

$$\mathbf{M}\Phi = \frac{1}{k_{\mathrm{eff}}}\mathbf{F}\Phi \qquad (2.5)$$

(**M** and **F** are migration and leakage and fission operators, and k_{eff} is the eigen value) while the absolute value of the neutron flux is determined by the reactor power (P) normalization:

$$P = \gamma \int_{V \in V_{\mathrm{CORE}}} \Sigma_f(x,y,z)\,\Phi(x,y,z)\,\mathrm{d}V = \sum_{m=1}^{M} Q_m \qquad (2.6)$$

Where it is clear that the core volume (V_{CORE}) and core average power density (q_{AVE}) can be written respectively as:

$$V_{\mathrm{CORE}} = \sum_{m=1}^{M} \int_{V \in V_m} \mathrm{d}V = \sum_{m=1}^{M} V_m \qquad (2.7)$$

$$q_{\mathrm{AVE}} = \frac{P}{V_{\mathrm{CORE}}} \qquad (2.8)$$

In this case, since the reactor is always operated under critical condition the k_{eff} is practically very close to unity. The criticality condition ($k_{\mathrm{eff}} = 1$) is controlled by the adjusting the insertion depth of the control rods into the core (where it is assumed here the rods are operated in a bank mode).

The time interval used in the integration of Eq. (2.6) can be chosen short enough such as that the Q_m can be considered to be constant. Q_m is renewed by new fission cross sections and new neutron flux distributions which depends on the burn-up level of each fuel element. In the exact (3-D) burn-up calculation model, the 3-D neutron flux distribution can be produced directly from the 3-D solution of Eq. (2.8), and in turn, the burn-up equation, Eq. (2.6), can be solved without any approximation.

2.3 Effects of Non-Fuel of the Core

Most of the research reactors presently utilizing HEU (high enriched Uranium) are being converted to MEU (medium enriched uranium) fuel, provided keeping its performance, power level and availability unchanged. This conversion process demands an increasing in U-235 content to compensate for the loss of reactivity due to the increased absorption of neutrons by U-238 percent. To increase the amount of uranium in each fuel one can either increase the volume of the part of fuel element occupied by uranium or one can increase the amount of uranium packed into the available volume.

The effect of reflector material such as graphite, beryllium on two dimensions flux distribution and excess reactivity of the core has been studied using standard computer codes Wims-D4 and Daixy.

The core was assumed to be reflected by single row of reflector material (graphite / Beryllium) on two opposite faces and surrounded by light water on all other sides. The advantages of using reflector are: To reduce the critical volume of the core and reactor, to reduce the critical mass of the fuel and to flatten and improve the average neutron flux, thus increasing the excess reactivity of the core. For studying the effect of different reflector material on multigroup neutron fluxes and core excess

relativities, the graphite reflector, the excess relativities added having slight advantage because of its higher slowing down power and moderation ratio. In other side, beryllium is best reflecting material due to higher slowing down power when compared with graphite, also average thermal neutron flux increases with slightly lower peak value in the reflector region. In the reflector region (graphite - beryllium) next to the fuel thermal flux recovers rapidly to the value in the HEU case and the flux is only the percent lower in a typical water-trap or irradiation position inside or outside the core**.**

Reflector materials better than light water in the order of priority are beryllium and graphite. The later will need canning if it is to be used in pool-type research reactors such canning will reduce the core excess reactivity and affect the flux shape to some extent. Thus beryllium, which adds maximum excess reactivity and does not, required canning proves to be the best reflector material and could be the first choice. Although the problem associated with beryllium such as its an availability and very high cost, which should be taken in consideration it is still the first choice. Graphite has good nuclear reflector characteristics and has been used in several researches and power reactors, as it's easily available and easy to fabricate. Finally, we conclude from the above points that the beryllium is a best reflector material than graphite. (Qasid, 2008).

2.4 Flux Distribution

In order for the power generated by fission reaction to be maintained at constant level, the fission rates most remain steady over the course of time. This means that the number of thermal neutrons that cause fission in one generation must be the same as those that cause fission in the next generation and the next, and so on. Thus, the total number of neutrons in the reactor must remain constant.

2.4.1 Neutron Flux Distribution in the Reactor.

The thermal neutron flux is the quantity determine by the fission rate cm^2 per second and thus, the power generated in the fuel. Due to the fact that the different at each point of the reactor, its distribution or form is of utmost importance, since it will determine the distribution of power generated in the core. In general the thermal neutron flux achieves its maximum value in the center of the reactor and falls to zero at the contour of the reactor, since no thermal neutron are produce in this area. The distribution of the neutron flux depends greatly on form of the reactor and since most of the reactors are cylindrical, we will discuss this form.

Considering flux distribution in two directions: axial and radial from the center of the reactor (Fig: 2.3)

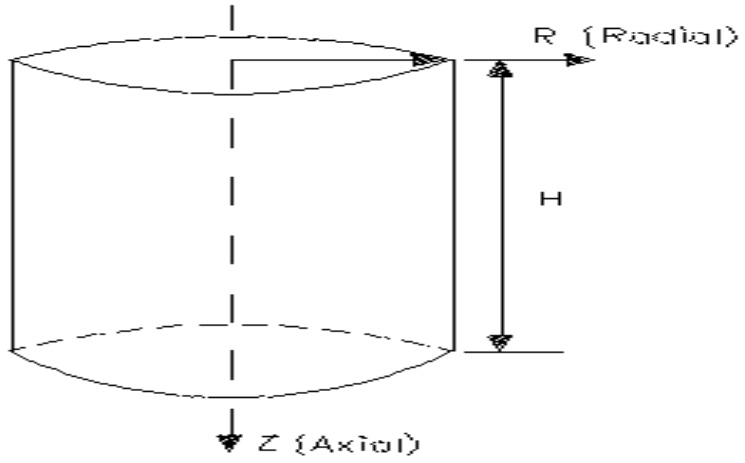


Fig 2.6: Is the axial and radial from the center of the reactor (module 10)

The form of the flux along the axes is provided in the following expressions:

Axial: (module 10)

$$\emptyset z = A \cos \frac{\pi Z}{H} \qquad (2.9)$$

Along the contour of the core (Fig.2.3), it is given that Z=H/2 and Z=-H/2, thus, it is given that t/2=0, therefore: U_z=0.

The distributions of the flux along the radius have a similar form. It is not exactly a cosine, but it is nevertheless, fairly correct to express it as (module 10)

$$\emptyset z = BJ_0\left[\frac{2.40r}{R}\right] \quad (2.10)$$

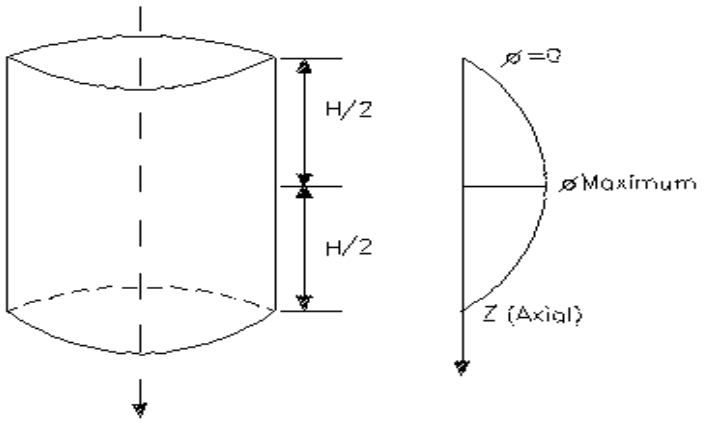


Fig. 2.7: Distributions of the flux along the radius

Along the contour (figure 2.3), it is given that r=R. therefore: U_z=0

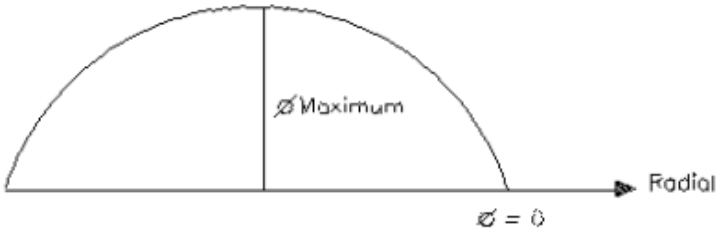


Fig: 2.8: Radial Distribution of a flux

One of the physical conditions is that U_z must not drop abruptly to zero along the geometry contours, but that it does so at a given distance (Figure 2.8).

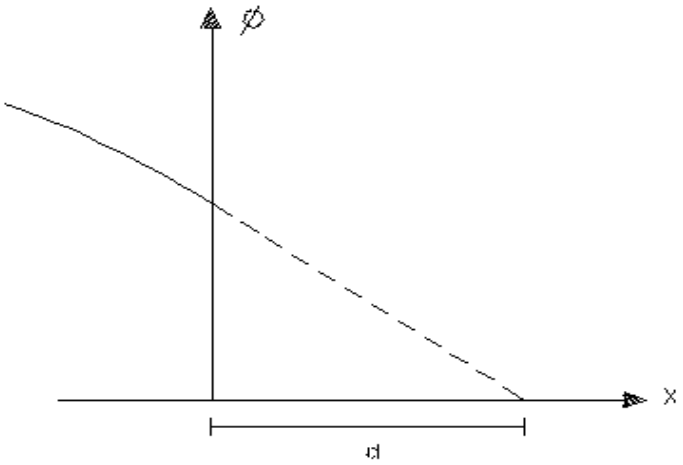


Fig: 2.9 a variation of flux and distance

Combining both distributions, we find that the flux is related to (Zr) at any given point in the reactor as: (module 10)

$$\emptyset_{z,r} = \emptyset_{max} \cos\frac{\pi z}{H} J_0 \left[\frac{2.405r}{R}\right] \qquad (2.11)$$

2.4.2 Implication for non-uniform Distribution of Flux.

As the neutron flux has a maximum value at the center of the reactor and drop to zero in the contours, the maximum neutron flux generated by the fuel will be produced at center of the reactor and very little power will be generated in the fuel located in the outer areas. The total power produced in the reactor will depend on the average thermal flux. Due to the type of distribution produce in a cylindrical reactor the average flux is only 27.5% of the maximum flux. (module 10)

$$\frac{\emptyset}{\emptyset_{max}} = \mathbf{27.5}\% \qquad (2.12)$$

The only way to increase the total power generated by the reactor, is by increasing the average flux. If we maintain the same flux distribution, the only way to augment the average flux is by increasing the maximum flux. (Fig: 2.8)

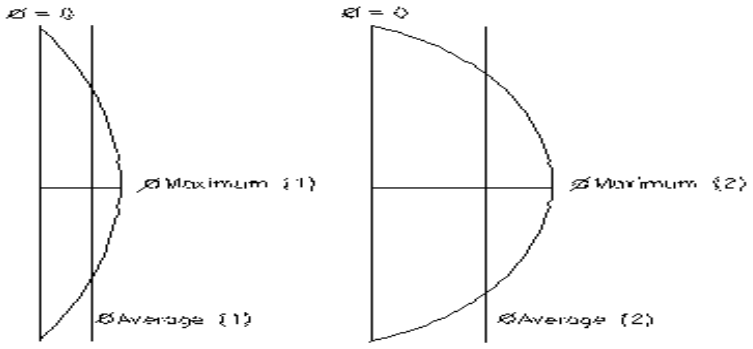


Fig: 2.10. Radial Distributions of the flux (module 10)

Nevertheless, this situation will increase the heat generated by the fuel in the center of the reactor and might not be accepted due to limit of the fuel and the heat extraction of the system. (module 10)

In the normal case where an assembly consists of only one kind of fuel rod of U^{235} enrichment, the corner fuel rod nearest to the cruciform water gap generates the highest power in the assembly. The ratio between the highest power and that average over the assembly is called the Power Peaking Factor (PPF), and is a key value that dictates the maximum allowable power density of the assembly. (module 10)

An important problem in the design of the fuel assembly is how to depress the local Power Peaking Factor. A commonly adopted expedient to flatten the power distribution is to use fuel rods that are allowed in enrichment at the corners. Limitation are imposed on this expedient by local Power Peaking produced at different position in the fuel assembly by excessive lowering of the enrichment at the corners, and by the impairment that would expected of the multiplication factor with the use of too many fuel rod with low enrichment. This calls for optimization of the enrichment distribution within individual fuel assemblies. (module 10)

2.5 POWER PEAKING FACTOR

The Power Peaking Factor represents the maximum power factor among all the fuel rod in the studied assembly. It is a relative power value which is calculated according to the below equation. The thermal hydraulic design of the Reactor Core is done for the maximum power (not only for the average power), thus it is better to use new quantity "Power Peaking Factor" which is define as: (Module 10, Vladimir *et al*. 2011)

PPF = (maximum power density)/ (average power density)

$$\boldsymbol{PPF = (P_{fuel} - P_{av})/P_{av}} \quad (2.13)$$

where, P_{fuel}= power in the specific fuel;

P_{av}= average power of the whole assembly.

PPF = power peaking factor.

Power Peaking Factor can be either positive or negative, and it clearly shows the power magnitude of each fuel rod.

The weighting factor for each type of the fuel assembly based on their fuel compositions, where the coupling codes were used to calculate the thermal power produced by each fuel assembly eqn (2.14): (Yashar *et al*., 2012)

$$C_i = \frac{P_i}{P_{ave}} \quad (2.14)$$

where C_i =: is the weighting factor value, i represent the type of fuel assemblies;

P_i=: is the produced thermal power in each type of fuel assembly; and

P_{ave}=: is the produced power of the fuel assembly with the averaged enrichment.

In order to calculate the weighting factor, we assumed an equal neutron flux in numerator and denominator of this formula; as a result, neutron flux parameter was removed from both the numerator and denominator of this correlation.

Then, to calculate the geometrical weighting factor (the "G" factor) of the m positions of the core, the whole reactor core was loaded based on the averaged fuel composition, and the radial power peaking factor was obtained from positions accordingly: (Yashar *et al.*, 2012)

$$G_m = 163 \frac{P_m}{\sum_{m=1}^{163} P_m} \tag{2.15}$$

where m = the number of fuel assemblies,

m=163 and

P_m= produced thermal power of each fuel assembly.

2.5.1 Fuel Temperature Coefficient of Reactivity

A negative temperature coefficient of reactivity (NTC) occur when the thermal conductivity of a material rises in increasing temperature of reactivity, typically in a define temperature range (Ahmed, *et al.*, 2011).

For most materials the thermal conductivity will decrease in increase in temperature. An important cause of transient change in the effective of multiplication factor in an operating reactor is variation of the change of the temperature of the system. Such variation may be localized example due to non-uniformity of structure affecting the flow of coolant at particular point, or they may affect the reactor as whole. A change in the rate of flow of coolant for example would gradually alter the temperature of the reaction. A similar effect may result from a change in power that is heat removed from the coolant, so that temperature at the latter re-enter the reactor would be change.

If the effective multiplicative factor (or reactivity) of a reactor were to be decrease with temperature that is if the temperature coefficient of reactivity where to be negative, then the transient increase in temperature will be accompanied by decrease in

reactivity. The rate of heat generated would then decrease thereby causing the temperature to fall. Similarly, if there where transient decrease the increase in reactivity would increase the rate of heat generation and tend to restore the original temperature. In such a reactor, temperature transient, either an increase or decrease, would be self-limiting. In a nuclear reactor, temperature change can introduce reactivity changes. This property is called the "temperature coefficient of reactivity". In water cooled nuclear reactor, the predominant reactivity is brought about changes in the temperature cause a decrease in reactivity. A temperature coefficient of reactivity, thus a desirable feature since it is an important factor in reactor stability and operational safety.

In reactivity induced accidents, the reactor power, after a reactivity insertion, the power has an exponential behavior given by:

$$P(t) = P_0 \exp\left[\int_0^t \frac{\dot{\rho}(t') + \lambda\rho(t')}{\beta - \rho(t')}\,\mathrm{d}t'\right] \tag{2.16}$$

In the absence of any control reactivity, the reactor power continues to increase exponentially. However, in the presence of feedback and control mechanisms, the reactivity $\rho(t)$ that drives the transient is the net effect of contributions arising from several mechanisms:

$$\rho(t) = \rho i(t) + \rho \mathrm{fb}(t) + \rho \mathrm{c}(t) + \rho \mathrm{sd}(t) \tag{2.17}$$

The feedback reactivity $\rho_{\mathrm{fb}}(t)$ depends on the fuel, clad and coolant temperatures as well as density coefficients for the reactor core. The reactivity feedback arising from the change in fuel temperature is called the prompt reactivity feedback since it directly follows the change in fuel temperature and no time delay is involved between the changing fuel temperature and production of feedback. The other feedbacks are called

the delayed feedbacks since some time delay is involved between the change in fuel temperature and occurrence of feedback.

β_{eff}=: effective delayed neutron fraction

Λ =: prompt neutron generation time

ρ_c =: reactivity from the reactor power control system

ρ_{fb}=: reactivity from thermal hydraulic feedback

ρ_i =: reactivity inserted by the initiating event

ρ_{sd}=: shutdown or trip reactivity

ρ_U =: uranium density in fuel

At low reactor power levels, changing the flow rate of the coolant through the reactor does not result in a measurable reactivity because fuel and moderator temperature and the fraction of the steam void occurring in the core are not changed appreciably. When the flow rate is varies, however, the temperature that occur across the core (outlet versus inlet temperature) will vary inversely with the flow rate (Ahmad, *et al*., 2011). At higher power levels, on liquid systems, increasing flow will lower fuel and coolant temperatures slightly, resulting in a small positive reactivity insertion. A positive reactivity addition also occurs when flow is increase in a two phase (steam water) cooled system. Increasing the flow rate decrease the fraction of steam voids in the coolant and result in a positive reactivity addition. Two main effects contribution to the fuel reactivity effect:

i) Doppler broadening.

Doppler effects are result of increased resonance capture reaction rate in U-238 due to resonance broadening (the same effect as in low enriched uranium power reactor). In reactor Doppler Effect contributes less than half to the total fuel temperature reactivity effect. Looking into the different reactivity feedbacks, it is seen

that the Doppler and moderator void/density feedback relativities increase as uranium density increases while the moderator temperature feedback reactivity decreases as uranium density increases. The net reactivity in the system rises above the 1$ mark making the reactor super prompt critical. For super prompt reactivity insertions in a critical reactor, the reactor period is approximately given by (IAEA-TECDOC-643, 1992)

$$T = \frac{\Lambda}{(\rho - 1)\beta_{\text{eff}}} \tag{2.17}$$

where, ρ is the reactivity insertion in dollars.

Thus, increasing β_{eff} is approximately equivalent to decreasing t Λ by the same amount (IAEA-TECDOC-643, 1992). Hence, the reactor with maximum Λ/βeff value will have maximum period hence minimum power rise due to reactivity insertion. Since reactor is very sensitive to changes in Λ and/or β_{eff} as shown in IAEA-TECDOC-643 (1992), and the reactor is not so sensitive to change in reactivity feedback, similar trend is reflected here, too. The minimum reactor period attained during the transient also shows the same trend.

ii) Thermal spectrum shifts (spectrum hardening).

Spectrum hardening is a dominating effect of the reactors. The effect is as follows: Increasing in fuel temperature result in shift to higher energy and deformation of Maxwellian spectrum in fuel. Spectrum in water is only slightly affected due to smaller increase in water temperature. Fission reaction rate in fuel is reduced. Ratio of fission reaction rate and absorption reaction rate (potential difference equal to multiplication factor) is reduced. Reactivity effects are negative.

2.5.2 Diffusion Theory Calculation.

A relatively simple description of neutron diffusion theory is a one-speed diffusion approach, which mathematically describes the nuclear reaction. Such approach has great advantage of illustrating many of the important features of nuclear reaction without the complexity that is introduced by treatment of important effects associated with the neutron energy spectrum and with highly directional neutron transport. Moreover, diffusion theory is sufficiently accurate in providing a quantitative understanding of many physics features of nuclear reactor.

According to Frick's law of diffusion, the net rate of neutron flow in a given direction is proportional to the negative partial gradient of the neutron flux. For a diffusion of one speed neutron in the Z- direction, Frick's law stated that (Ahmed, *et al.*, 2008):

$$J_Z = -D\frac{\partial \Phi}{\partial Z} \qquad (2.18)$$

where: $\frac{\partial \Phi}{\partial Z}$: = neutron flux gradient in Z direction

J_Z = the current density in this direction

D = the neutron diffusion coefficient.

The negative sign take account of the fact that the diffusion process is in a direction opposite to that of increasing neutron density.

The diffusion coefficient is given from kinetic equation as

$$D = \lambda_{tr} \frac{V}{3} \tag{2.26}$$

where, λ_{tr}= is the transports mean free path, V, the appropriate neutron velocity.

The diffusion coefficient has the dimension of length is usually express in meters. In order to take into consideration neutron diffusion in all directions, the Frick's law is written in general form as: (fick's law of diffusion)

$$J = -Dgrad\Phi = -D\nabla\Phi \tag{2.19}$$

Inserting the neutron current density J to the given one speed neutron balance equation and rearrenging we have:

$$\nabla[D\nabla\Phi(r,t)] - \sum_a \Phi(r,t) + S(r,t) = \frac{\partial n(r,t)}{\partial t} \tag{2.20}$$

If the system is homogeneous, the diffusion coefficient is independent of position. In this circumstance, the neutron leakage term becomes:

$$\nabla[D\nabla\Phi(r,t)] = D\nabla^2\Phi(r,t) \tag{2.21}$$

The diffusion equation is writen in the form:

$$D\nabla^2\Phi(r,t) - \sum_a \Phi(r,t) + S(r,t) = \frac{\partial n(r,t)}{\partial t} \tag{2.22}$$

When a stable state is establish, the neutron density "n" at any given point inside the moderator will no longer vary with time "t". we can therefore, say that $\frac{\partial n(r,t)}{\partial t} = 0$ and the neutron production is then exactly balanced by the combined losses due to leakage and absorption.

The steady state diffusion equation for one speed neutron is consequently:

$$D\nabla^2\Phi(r) - \sum_a \Phi(r) + S(r) = 0 \tag{2.23}$$

In a non multiplying media, i.e. the one containing no fissile material, the source term "S" in a steady state diffusion equation is zero except in the actual position of the

neutron source. Then the diffusion is solve by setting S=0 at all point in the medium outside the source. If S=0 the steady state diffusion equation in a non multiplying medium reduces to the homogeneous form applicable anywhere except at the source, this is:

$$D\nabla^2\Phi(r) - \sum_a \Phi(r) = 0 \qquad (2.26)$$

Define the diffusion length "L" of the one speed neutrons is in the given diffusion medium as:

$$L = \sqrt{\frac{D}{\Sigma_a}} \qquad (2.26)$$

Inserting diffusion length "L" into diffusion equation in a non multiplying media and rearrenging we have:

$$\nabla^2\Phi(r) = \frac{1}{L^2}\Phi(r) = 0 \qquad (2.27)$$

This equation has the same form as the helmholtz equation and is often referred to by this name.

The procedure for solving the equation in a simple will be illustrated by reference to the one speed neutron from a point source into an infinite non multiplying medium. For a point source in an infinite medium, the neutron distribution may be regarded as having spherical coordinates, the source free diffusion equation becomes:

$$\boldsymbol{\frac{d^2\Phi(r)}{dr^2} + \frac{2}{r}\frac{d\Phi(r)}{dr} - \frac{1}{L^2}\Phi(r) = 0} \qquad (2.28)$$

To solve this equation , we reduce the variable $\Phi = y/r$, so that the above equation reduces to:

$$\frac{d^2y}{dr^2} - \frac{1}{L^2}y = 0 \qquad (2.29)$$

Since the diffusion length L^2 is a positive quantity, the general solution of the above equation is:

$$y = Ae^{-\frac{r}{L}} + Ce^{\frac{r}{L}} \quad (2.30)$$

And hence $\Phi(r) = A\frac{e^{-\frac{r}{L}}}{r} + C\frac{e^{\frac{r}{L}}}{r}$ (2.31)

The constant A and C are determine by boundary conditions. If C is not equal to zero, then the flux became infinite as $r \to infinity$. since the flux must be always finite, except at the origin, its follows that C must be zero, the general solution applicable to present case reduces to:

$$\Phi(r) = A\frac{e^{-\frac{r}{L}}}{r} \quad (2.32)$$

To evaluate A, the so called source condition is used. If J is the neutron current density at the surface of the sphere of radius r, with the source at the center,then the total number of neutrons passing through the whole of the surface per second will be $4\pi r^2 J$. The limiting value of this number as r approaches zero will be equal to the source strength S neutron per second i.e. to the total number of neutrons emitted by the point source in all directions per second. Thus:

$S = \lim_{r\to 0} 4\pi r^2 J$ (2.33)

Define J as $J = -D\frac{\partial \Phi}{\partial r}$ (2.34)

It therefore implies that $J = DAe^{-\frac{r}{L}}\left(\frac{1+\frac{r}{L}}{r^2}\right)$ so that we have

$S = \lim_{r\to 0} 4\pi r^2 \, DAe^{-\frac{r}{L}}\left(\frac{1+\frac{r}{L}}{r^2}\right)$ (2.35)

And hence as $r \to 0$ we have

$S = 4\pi r^2 DA + 0 \; or \; A = \frac{S}{4\pi D}$ (2.36)

Subtituting the value of "A" in the general solution above, we get:

$\Phi(r) = \frac{S}{4\pi D}.\frac{e^{-\frac{r}{L}}}{r}$ (2.37)

Where D is the diffusion coefficient, S is the source strenght neutron per second, and L is the diffusion length.

2.6 Heat Transfer Model

2.6.1. Heat Transfer Correlation Model

Based on the flow chart of supercritical-pressure light water reactor, Watts correlation is chosen for the calculation of convective heat transfer coefficient in which descending flow and ascending flow are respectively considered. It can be expressed from the following equations: (Rahul *et al*., 2009)

(a) For ascending flow

$$Nu = \begin{cases} Nu_{varp} & \frac{\overline{Gr_b}}{Re_b^{2.7}\overline{Pr_b}^{0.5}} < 10^{-5} \\ Nu_{varp}\left(1 - \frac{3000\overline{Gr_b}}{Re_b^{2.7}\overline{Pr_b}^{0.5}}\right)^{0.295} & 10^{-4} \leqslant \frac{\overline{Gr_b}}{Re_b^{2.7}\overline{Pr_b}^{0.5}} \\ Nu_{varp}\left(\frac{7000\overline{Gr_b}}{Re_b^{2.7}\overline{Pr_b}^{0.5}}\right)^{0.295} & 10^{-5} \leqslant \frac{\overline{Gr_b}}{Re_b^{2.7}\overline{Pr_b}^{0.5}} < 10^{-4} \end{cases} \quad (2.38)$$

(b) For descending flow

$$Nu = Nu_{varp}\left(1 + \frac{30000\overline{Gr_b}}{Re_b^{2.7}\overline{Pr_b}^{0.5}}\right)^{0.295} \quad (2.39)$$

where

$$Nu_{varp} = 0.021 Re_b^{0.8}\overline{Pr_b}^{0.55}\left(\frac{\rho_w}{\rho_b}\right)^{0.35}; \quad \overline{Gr_b} = \frac{(\rho_b - \bar{\rho})gD_e^3}{\rho_b \mu_b^2};$$
$$\overline{Pr_b} = \frac{\overline{C_p}\mu_b}{k_b}; \quad \bar{\rho} = \frac{\int_{T_b}^{T_p}\rho dT}{T_p - T_b}; \quad \overline{C_p} = \frac{\int_{T_b}^{T_p} C_p dT}{T_p - T_b} = \frac{h_p - h_b}{T_p - T_b} \quad (2.40)$$

where, *Nu*= is Nusselt number

.Re_b= is Reynolds of coolant or moderator.

$\overline{Pr_b}, \overline{Gr_b}$ = are respectively Prandtl number and Grashof number.

ρ_w, ρ_b= are respectively wall density and fluid density in flow channels, in kg/m^3.

T_p, T_b= are respectively wall temperature and fluid temperature in flow channels, in °C.

h_p, h_b= are respectively wall enthalpy and fluid enthalpy in flow channels, in kJ/kg.

D_e= is the equivalent diameter of fuel channels or moderator channels, in m.

k_b= is the heat conductivity of coolant or moderator, in W/(m K).

μ_b= is the dynamic viscosity of coolant or moderator, in (N.s/m^2).

2.6.2 Heat Transfer Model between Fuel Cladding, Coolant and Moderator

It includes a series of heat transfer process: heat conduction of fuel cladding, convection heat transfer between fuel cladding and coolant, convection heat transfer between coolant and water rod wall, and so on. The calculation model is shown in the following equation:

$$Q = (T1 - T2)/\Sigma R \qquad (2.41)$$

In which,

Q= is the heat released from fuel rods or the heat passed through water rod wall, in W.

T_1, T_2= are respectively the start site and the end site of heat transfer process, in °C.

ΣR = is the heat flow resistance, which is calculated by the heat conductivity convective heat transfer coefficient and heat exchange area, W/ (°C).

The heat conductivity coefficient is calculated by means of simultaneous solutions of Eqs. (2.42),

$$h = \frac{kNu}{D_e} \qquad (2.42)$$

where

h= is the heat conductivity coefficient between fuel cladding and coolant, or between water rod wall and coolant/moderator, W/(m^2 K).

k= is thermal conductivity, W/(m K).

Thermal conductivity of fuel element cladding and stainless steel layer of water rod wall is taken as 20.4 W/(m K), and thermal conductivity of heat insulation layer is taken as 0.5 W/(m K).

CHAPTER THREE

METHODOLOGY

3.0 Methods

Reactor safety demands that more than one safety features measurements are to be adopted in the study of reactor power and flux distribution. This has been shown by recent workers in the field of safety and thermal behavior of MNSR (Balogun, 2003, Ahmed, *et al*. 2006, Jonah, *et al*. 2007, Ahmed, *et al*. 2010, Musa, *et al*. 2011, Ahmed, *et al*. 2012, Ahmed, *et al*. 2013.). In this work, the thermal hydraulic and rod positions parameters (dependent on equation 3.3 and 3.4) were used.

3.1 Computer Program.

A program was developed using Netbeans IDE 7.4 software based on temperature difference and control rod movement equation of power (equation 3.3 and 3.4 respectively) below. Details of the program are in Appendix A.

3.2 Determination of Power Peaking Factor and Thermal Limitation of NIRR-1

3.2.1 Temperature difference method

The equation that depicts the relation amongst core inlet temperature, temperature difference and power level as obtained from simulation experiment on MNSR is expressed in the form (Shi, 1990)

$$\Delta T = (5.725 + 147.6H^{-2.64})T_i^{-0.35}P^{(0.59+0.0019T_i)} \quad (3.1)$$

where ΔT =temperature different between the inlet and outlet orifice ^{0}C

H= Hieght of the inlet orifice (mm) and have a constant value of 232mm

T_i = inlet temperature ^{o}C

The designed of the inlet orifice of NIRR-1 was made to be 6mm for safety and technical reason (yang, 1990). Therefore subtituting the value of H into equation (3.1) reduces the equation to:

$$\Delta T = 7.04 T_i^{-0.35} P^{(0.59+0.0019T_i)} \quad (3.2)$$

$$\text{Thus } P = Exp\left[Ln\left(\frac{\Delta T}{7.04T_i^{-0.35}}\right)\left((0.59 + 0.0019T_i)\right)^{-1}\right] \quad (3.3)$$

For a fixed height of inlet orifice, it is expected from equation 3.3 that the reactor power varies linearly with temperature.

3.2.2. Control rod movement method

Apart from the above method of determining the power of the reactor via thermal hydraulic parameters, (neutron flux values) could as well be exploited to predict the flux distribution of the reactor, as long as nuclear parameter are accurately known (Ahmed *et. al*. 2008) the equation that relate these two parameter obeys the following relation:

$$P = 3.1 \times 10^{-10} \sum_f V_f \emptyset \quad (3.4)$$

Where φ= average thermal neutron flux in the inner irradiation channel (n cm^{-2}/s)

V_f = volume of the core = $\Pi r^2 h$ (cm^3)

Core height (h)=23.00cm

Core radius (r) = 11.5cm

$\sum_f$ = macroscopic cross section of the core fuel =$1.013\times10^{-2}cm^{-1}$

P= Power of Reactor in kW

A core dimension of 23.00cm square cylinder and highly enriched uranium was used as fuel for the Nigerian MNSR. The above parameter make it possible to reduce the equation (3.4) to only flux dependent parameter as shown in equation (3.5)

$$P = 3.0 \times 10^{-8} \emptyset \quad (3.5)$$

Equation (3.5) reveals a linear relationship between the reactor power and its neutron flux.

The Power Peaking Factor for each type of the fuel assembly based on their fuel compositions, where the coupling codes were used to calculate the thermal power produced by each fuel assembly. The equation below gives the maximum power factor produce in reactor core

The Power Peaking Factor for each type of the fuel assembly based on their fuel compositions, where the coupling codes were used to calculate the thermal power produced by each fuel assembly. The equation below gives the maximum power factor produce in reactor core: (Yashar *et al*., 2012))

$$PPF = {}^{P_i}/_{P_{ave}} \quad (3.6)$$

where: *PPF* = Power Peaking Factor

P_i = is the thermal power produced in the fuel assembly (kW) and

P_{ave} = is the preset power of the fuel assembly (kW).

We applied equation (3.1) and (3.4) in this work to determine the Power Peaking Factor and thermal Limitation of Nigerian Research Reactor – 1 core performance. The Reactor was operated at a preset flux value of 5×10^{11} n cm^{-2} s^{-1} and the control rod position limited to 22.00 cm. This is to make the reactor operate at half power (15 kW) ofits expected installed capacity.

When the Reactor was operating at the preset flux value, the inlet , outlet temperatures of the coolant and control rod position were recorded after every twenty minute for different durations of operation. The results obtained shown in table (4.1 – 4.10), from wherethe temperature differences were evaluated. This enabledthe investigation of the following:

a) fairly constant reactor power and flux distribution with temperature difference.
b) the temperature difference recorded during the operation is fairly constant with time.
c) steady rise in the inlet and outlet temperature with time.
d) there is insufficient thermal circulation of coolant in the core.
e) the control rod position will rise gradually with time to compensate for high negative temperature coefficient of reactivity
f) the control rod movement will satisfy one of the safety requirement of the reactor, which does not permit unnecessary power excursion and occurrence of boiling.
g) the Reactor power will be kept at the initial preset level

The Power Peaking Factors were obtained with the reactor operating at the same preset flux but varying operational times to establish stability of the reactor over time as proclaimed by the Reactor vendors and as shows by many researchers (Balogun, 2003, Jonah *et al*., 2007, Ahmed, *et al*., 2010, Ahmed, *et al*., 2011, Musa, *et al*., 2012, Ahmed, *et al*., 2013) in the area of Miniature Neutron Source Reactors.

CHAPTER FOUR

(Results and Discussion)

4.1 Results

The results obtained in this work are hereby presented in tables 4.1 to 4.10 below. All measurements were done at a preset flux value of 5×10^{11} n cm^2 $s^{-1}$and preset power of 15 kW. This is done in order to study the contribution of temperature coefficient of reactivity on the Reactor power stability.

Table 4.1: Reactor Power Peaking Factor obtained using measured coolant temperature rise for 1hr

Clock Time (Hrs)	Inlet Temperature (˚C)	Outlet Temperature (˚C)	Coolant Temperature (˚C)	Predicted Power (kW)	**Power Peaking Factor**	Standard deviation	Percentage Error %
1.5	24.2	24.5	0.30	0.0404	**0.0027**	0.9973	99.73
1.6	24.1	37.1	13.0	15.1271	**1.0085**	-0.0085	0.85
1.8	26.0	38.9	12.9	15.3423	**1.0228**	-0.0228	2.28
2.0	27.0	40.1	13.1	15.9126	**1.0608**	-0.0608	6.08
2.2	28.4	40.6	12.2	14.4779	**0.9652**	0.0348	3.48
2.4	28.9	40.6	12.6	15.3051	**1.0203**	-0.0203	2.03
2.4	28.6	41.3	12.7	15.4437	**1.0296**	-0.0296	2.96
2.4	29.1	33.3	4.20	2.7949	**0.1863**	0.8137	81.37
Average	27.0	37.0	10.1	10.6075	**0.7072**	0.2928	29.28

Table 4.2: Reactor Power Peaking Factor obtained using measured coolant temperature rise for 6hrs

Clock Time (Hrs)	Inlet Temperature (˚C)	Outlet Temperature (˚C)	Coolant Temperature (˚C)	Predicted Power (kW)	**Power Peaking Factor**	Standard deviation	Percentage Error %
09:50	26.3	38.4	12.1	13.9352	**0.9290**	0.0710	7.10
10:10	27.9	40.4	12.5	14.9496	**0.9966**	0.0034	0.34
10:30	29.3	41.7	12.4	14.9939	**0.9996**	0.0004	0.04
10:50	30.1	42.3	12.2	14.7424	**0.9828**	0.0172	1.72
11:10	30.2	42.7	12.5	15.3215	**1.0214**	-0.0214	2.14
11:30	31.6	44.0	12.4	15.3349	**1.0223**	-0.0223	2.23
11:50	31.9	43.9	12.0	14.6205	**0.9747**	0.0253	2.53
12:10	32.1	44.2	12.1	14.8346	**0.9890**	0.0110	1.10
12:30	32.2	44.1	11.9	14.4726	**0.9648**	0.0352	3.52
12:50	31.5	44.3	12.8	16.0880	**1.0725**	-0.0725	7.25
13:10	32.6	44.4	11.8	14.3367	**0.9558**	0.0442	4.42
13:30	32.7	45.2	12.5	15.6749	**1.0450**	-0.0450	4.50
13:50	32.2	44.1	11.9	14.4726	**0.9648**	0.0352	3.52
14:10	32.6	44.7	12.1	14.8996	**0.9933**	0.0067	0.67
14:30	32.6	44.9	12.3	15.2790	**1.0186**	-0.0186	1.86
14:50	33.0	44.9	11.9	14.5733	**0.9716**	0.0284	2.84
15:10	33.3	45.0	11.7	14.2357	**0.9490**	0.0510	5.10
15:30	33.1	45.2	12.1	14.9627	**0.9975**	0.0025	0.25
15:50	33.3	45.1	11.8	14.4224	**0.9615**	0.0385	3.85
Average	31.5	43.7	12.2	14.9423	**0.9962**	0.0038	0.38

Table 4.3: Reactor Power Peaking Factor obtained using measured coolant temperature rise for 6hrs

Clock Time (Hrs)	Inlet Temperature (˚C)	Outlet Temperature (˚C)	Coolant Temperature (˚C)	Predicted Power (kW)	**Power Peaking Factor**	Standard deviation	Percentage Error %
10:15	25.0	37.6	11.6	12.8147	**0.8543**	0.1457	14.57
10:40	27.6	39.9	12.3	14.5282	**0.9685**	0.0315	3.15
11:00	28.8	40.9	12.1	14.3579	**0.9572**	0.0428	4.28
11:20	29.8	41.8	12.0	14.3265	**0.9551**	0.0449	4.49
11:40	31.1	42.6	12.5	15.4545	**1.0303**	-0.0303	3.03
12:00	30.0	42.9	12.9	16.0538	**1.0703**	-0.0703	7.03
12:20	31.4	43.3	11.9	14.3673	**0.9578**	0.0422	4.22
12:40	31.4	43.4	12.0	14.5535	**0.9702**	0.0298	2.98
13:00	31.3	43.9	12.6	15.6743	**1.0450**	-0.0450	4.50
13:20	31.1	43.6	12.1	14.6992	**0.9799**	0.0201	2.01
13:40	31.3	43.6	12.1	14.7269	**0.9818**	0.0182	1.82
14:00	32.4	43.4	12.2	15.0629	**1.0042**	-0.0042	0.42
14:20	33.7	44.6	11.7	14.2829	**0.9522**	0.0478	4.78
14:40	32.2	44.4	12.3	15.2263	**1.0151**	-0.0151	1.51
15:00	32.5	44.5	11.7	14.1384	**0.9426**	0.0574	5.74
15:20	32.6	44.4	11.6	13.9657	**0.9310**	0.0690	6.90
15:40	33.0	44.8	11.8	14.3861	**0.9591**	0.0409	4.09
16:00	32.8	45.5	12.2	15.1145	**1.0076**	-0.0076	0.76
16:20	32.8	44.7	11.9	14.5360	**0.9691**	0.0309	3.09
Average	32.7	43.1	12.1	14.9123	**0.9942**	0.0058	0.58

Table 4.4: Reactor Power Peaking Factor obtained using measured coolant temperature rise for 6hrs

Clock Time (Hrs)	Inlet Temperature (˚C)	Outlet Temperature (˚C)	Coolant Temperature (˚C)	Predicted Power (kW)	**Power peaking factor**	Standard deviation	Percentage Error %
11:00	28.3	40.5	12.2	14.4616	**0.9641**	0.0386	3.86
11:20	30.2	42.3	12.1	14.5707	**0.9714**	0.0286	2.86
11:40	30.9	43.3	12.4	15.2357	**1.0157**	-0.0157	1.57
12:00	32.5	44.7	12.2	15.0759	**1.0051**	-0.0051	0.51
12:20	33.4	44.8	11.4	13.6924	**0.9128**	0.0872	8.72
12:40	33.1	45.3	12.2	15.1525	**1.0102**	-0.0102	1.02
13:00	33.7	46.0	12.3	15.4178	**1.0279**	-0.0279	2.79
13:20	33.9	45.8	11.9	14.6814	**0.9788**	0.0212	2.12
13:40	34.3	46.4	12.1	15.1072	**1.0071**	-0.0071	0.71
14:00	34.2	46.0	11.8	14.5278	**0.9685**	0.0315	3.15
14:20	34.5	46.9	11.4	13.8156	**0.9210**	0.0790	7.90
14:40	34.4	47.1	12.7	16.2775	**1.0852**	-0.0852	8.52
15:00	35.1	46.8	11.7	14.4397	**0.9626**	0.0374	3.47
15:20	33.5	47.0	12.5	15.7778	**1.0519**	0.0519	5.19
15:40	34.7	46.7	12.0	14.9627	**0.9975**	0.0025	0.25
16:00	35.9	47.5	12.6	16.2848	**1.0837**	-0.0837	8.37
16:20	35.3	47.6	12.3	15.6048	**1.0403**	-0.0403	4.03
16:40	35.4	47.8	12.4	15.8095	**1.0540**	-0.0540	5.38
17:00	35.3	47.7	12.4	15.7983	**1.0532**	-0.0532	5.32
Avr	33.6	45.8	12.2	15.2144	**1.0143**	-0.0140	1.43

Table 4.5: Reactor Power Peaking Factor obtained using measured coolant temperature rise for 6hrs

Clock Time (Hrs)	Inlet Temperature (˚C)	Outlet Temperature (˚C)	Coolant Temperature (˚C)	Predicted Power (kW)	**Power Peaking Factor**	Standard deviation	Percentage Error %

11:50	28.7	40.8	12.1	14.3421	**0.9561**	0.0439	4.39
12:10	28.6	41.5	12.9	15.8227	**1.0548**	-0.0548	5.48
12:30	30.0	42.2	12.2	14.7275	**0.9818**	0.0182	1.82
12:50	30.7	42.8	12.1	14.6429	**0.9761**	0.0239	2.39
13:10	31.4	42.9	11.5	13.6307	**0.9082**	0.0918	9.18
13:30	32.0	44.3	12.3	15.1995	**1.0133**	-0.0133	1.33
13:50	31.8	44.5	12.7	15.9376	**1.0625**	-0.0625	6.25
14:10	31.2	44.6	13.4	17.2172	**1.1478**	-0.1478	14.78
14:30	32.1	44.4	12.3	15.2130	**1.0142**	-0.0142	1.42
14:50	32.5	45.0	13.5	17.6098	**1.1740**	-0.1740	17.4
15:10	33.5	44.9	11.4	13.7039	**0.9136**	0.0864	8.64
15:30	33.2	45.3	12.1	14.9751	**0.9983**	0.0017	0.17
15:50	33.0	45.0	12.0	14.7613	**0.9841**	0.0159	1.59
16:10	33.0	45.4	12.4	15.5219	**1.0348**	-0.0348	3.48
16:30	34.0	45.3	11.3	13.5767	**0.9651**	0.0349	3.49
16:50	34.1	44.1	10.0	11.2740	**0.7516**	0.2484	24.84
17:10	33.7	45.8	12.1	15.0362	**1.0024**	0.0024	0.24
17:30	34.8	46.4	11.6	14.2199	**0.9480**	0.0520	5.20
17:50	34.1	46.5	12.4	15.6586	**1.0439**	-0.0439	4.39
Avr	32.2	44.3	12.1	14.8478	**0.9899**	0.0101	1.01

Table 4.6: Reactor Power Peaking Factor obtained using measured coolant temperature rise for 6hrs

Clock Time (Hrs)	Inlet Temperature (˚C)	Outlet Temperature (˚C)	Coolant Temperature (˚C)	Predicted Power (kW)	**Power Peaking Factor**	Standard deviation	Percentage Error %
10:50	27.3	40.6	13.3	16.3509	**1.0901**	-0.0901	9.01
11:00	29.0	40.9	11.9	14.0223	**0.9348**	0.0652	6.52
11:10	29.9	42.8	12.9	16.0379	**1.0692**	-0.0692	6.92
11:20	30.8	41.8	11.0	12.6538	**0.8436**	0.1564	15.64
11:30	30.5	43.2	12.7	15.7477	**1.0498**	-0.0498	4.98
11:40	31.9	43.4	11.5	13.6947	**0.9130**	0.0870	8.70
11:50	31.5	43.9	12.4	15.3209	**1.0214**	-0.0214	2.14
12:00	31.8	44.3	12.5	15.5534	**1.0369**	-0.0369	3.69
12:10	32.9	44.8	11.9	14.5609	**0.9707**	0.0293	2.93
12:20	33.5	45.5	12.0	14.8226	**0.9882**	0.0118	1.18
12:30	32.8	45.4	12.6	14.8808	**1.0587**	-0.0587	5.87
12:40	33.4	45.1	11.7	14.2476	**0.9498**	0.0502	5.02
12:50	33.7	45.1	11.4	13.7267	**0.9151**	0.0849	8.49
Average	31.5	43.7	12.2	14.9423	**0.9962**	0.0038	0.38

Table 4.7: Reactor Power Peaking Factor obtained using different control rod position in cm

S/No	Rod Position (cm)	Predicted power (kW)	**power peaking factor**
1	0.00	0.0000	**0.0000**
2	1.00	0.6526	**0.0833**
3	2.00	1.3052	**0.1667**
4	3.00	1.9579	**0.2500**
5	4.00	2.6104	**0.3333**
6	5.00	3.2631	**0.4167**
7	6.00	3.9157	**0.5000**
8	7.00	4.5684	**0.5833**
9	8.00	5.2210	**0.6667**
10	9.00	5.8740	**0.7500**
11	10.00	6.5262	**0.8333**
12	11.00	7.1788	**0.9166**
13	12.00	7.8315	**1.0000**
14	13.00	8.4841	**1.0833**
15	14.00	9.1367	**1.1667**
16	15.00	9.7893	**1.2500**
17	16.00	10.4419	**1.3333**
18	17.00	11.0946	**1.4167**
19	18.00	11.7472	**1.5000**
20	19.00	12.3998	**1.5833**
21	20.00	13.0524	**1.6667**
22	21.00	13.7051	**1.7500**
23	22.00	14.3577	**1.8333**
24	23.00	15.0103	**1.9167**
Average	12.00	7.8315	**0.8740**

Table 4.8: Reactor Power Peaking Factor obtained using measured control rod position for full withdrawal

Radius of the core (cm)	Rod position (cm)	Predicted Power (kW)	Power Peaking Factor
0.00	0.00	0.000	0.000
1.00	1.00	0.005	0.001
2.00	3.00	0.059	0.013
3.00	5.00	0.222	0.048
4.00	7.00	0.553	0.120
5.00	9.00	1.110	0.240
6.00	11.00	1.954	0.423
7.00	13.00	3.143	0.680
8.00	15.00	4.737	1.024
9.00	17.00	6.795	1.469
10.00	19.00	9.376	2.027
11.00	21.00	12.539	2.711
11.50	23.00	15.010	6.491
11.50	23.00	15.010	6.491
11.00	21.00	12.539	2.711
10.00	19.00	9.376	2.027
9.00	17.00	6.795	1.469
8.00	15.00	4.737	1.024
7.00	13.00	3.143	0.680
6.00	11.00	1.954	0.423
5.00	9.00	1.110	0.240
4.00	7.00	0.553	0.120
3.00	5.00	0.222	0.048
2.00	3.00	0.059	0.013
1.00	1.00	0.005	0.001
0.00	0.00	0.000	0.000

Table 4.9: Reactor Power Peaking Factor obtained using measured control rod position for 6hrs

S/No	Clock Time (Hrs)	Rod position (cm)	Predicted Power (kW)	**Power Peaking Factor**
1	10:15	11.90	7.7662	**0.8667**
2	10:40	12.50	8.1578	**0.9104**
3	11:00	12.70	8.2883	**0.9250**
4	11:20	13.00	8.4841	**0.9468**
5	11:40	13.20	8.6146	**0.9614**
6	12:00	13.40	8.7451	**0.9760**
7	12:20	13.60	8.8757	**0.9905**
8	12:40	13.70	8.9409	**0.9978**
9	13:00	13.80	9.0062	**1.0051**
10	13:20	14.00	9.1367	**1.0197**
11	13:40	14.10	9.2020	**1.0269**
12	14:00	14.10	9.2020	**1.0269**
13	14:20	14.20	9.2672	**1.0342**
14	14:40	14.40	9.3978	**1.0488**
15	15:00	14.30	9.3325	**1.0415**
16	15:20	14.30	9.3325	**1.0415**
17	15:40	14.40	9.3978	**1.0488**
18	16:00	14.50	9.4630	**1.0561**
19	16:20	14.90	9.7241	**1.0852**
Average		13.73	8.9605	**1.0000**

Table 4.10: Reactor Power Peaking Factor obtained using measured control rod position for 6hrs

S/No	Clock Time (Hrs)	Rod position (cm)	Predicted Power (kW)	**Power Peaking Factor**
1	09:50	12.20	7.9620	**0.8841**
2	10:10	12.50	8.1578	**0.9058**
3	10:30	12.70	8.2883	**0.9203**
4	10:50	13.20	8.6146	**0.9565**
5	11:10	13.40	8.7451	**0.9710**
6	11:30	13.50	8.8104	**0.9783**
7	11:50	13.70	8.9409	**0.9928**
8	12:10	13.90	9.0714	**1.0072**
9	12:30	14.10	9.2020	**1.0217**
10	12:50	14.10	9.2020	**1.0217**
11	13:10	14.20	9.2672	**1.0290**
12	13:30	14.20	9.2672	**1.0290**
13	13:50	14.30	9.3325	**1.0362**
14	14:10	14.35	9.3651	**1.0399**
15	14:30	14.40	9.3978	**1.0435**
16	14:50	14.50	9.4630	**1.0507**
17	15:10	14.70	9.5935	**1.0652**
18	15:30	14.90	9.7241	**1.0797**
19	15:50	15.10	9.8546	**1.0942**
Average		13.80	9.0062	**1.0000**

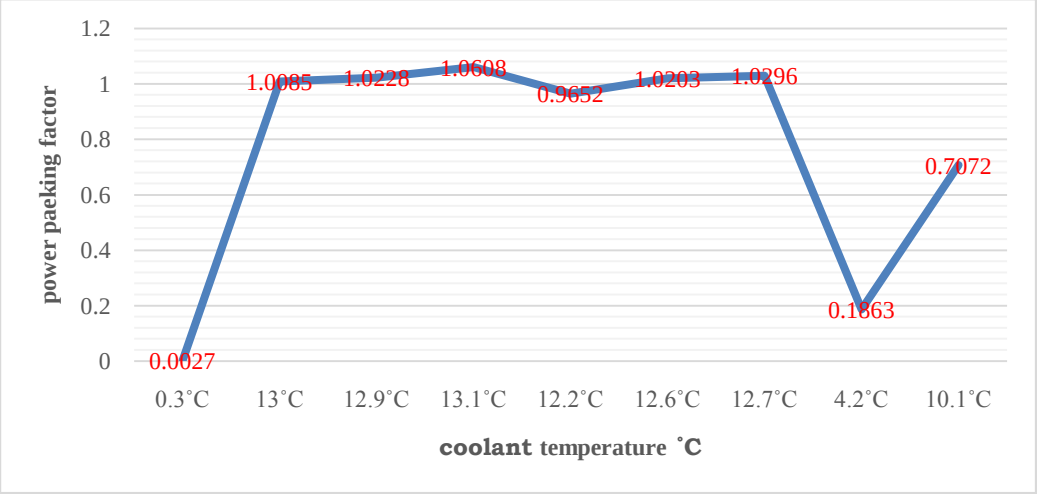


Fig. 4.1: Reactor Power Peaking Factor obtained using measured coolant temperature rise for 1hr

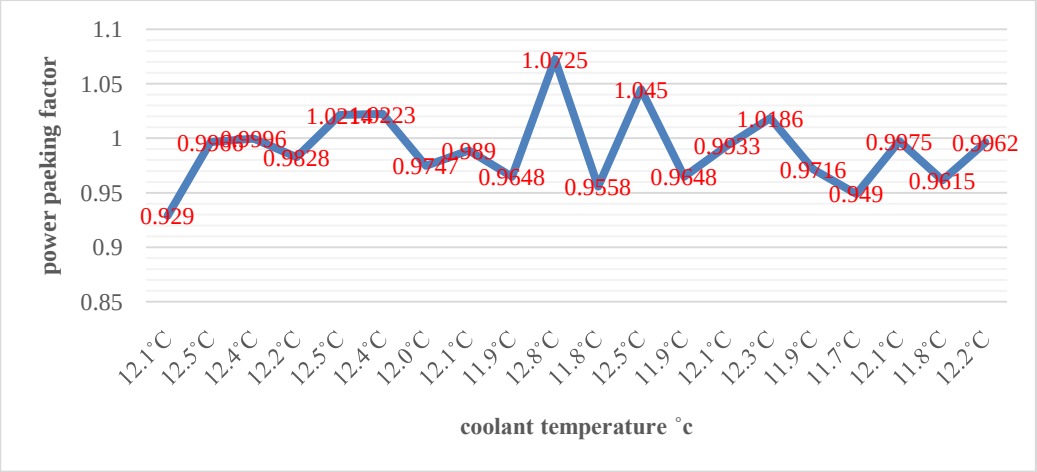


Fig. 4.2: Reactor Power Peaking Factor obtained using measured coolant temperature rise for 6hrs

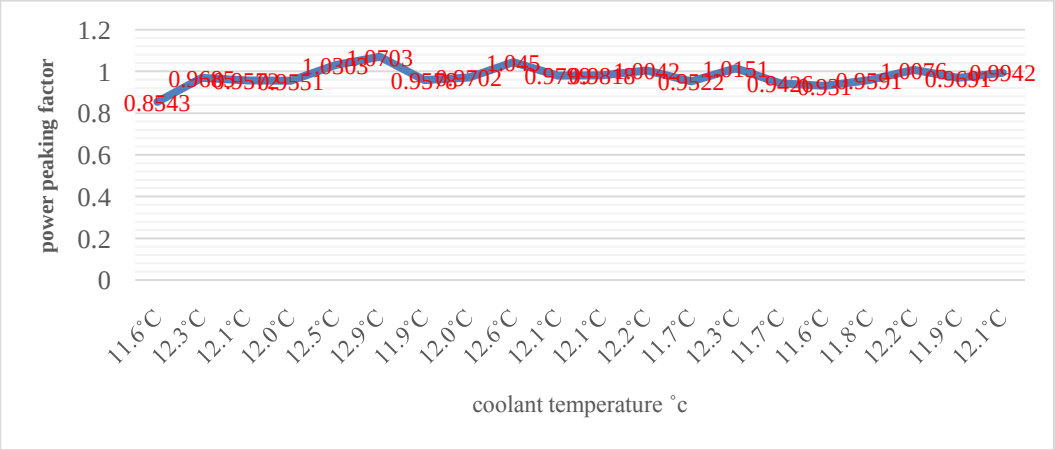


Fig. 4.3: Reactor Power Peaking Factor obtained using measured coolant temperature rise for 6hrs

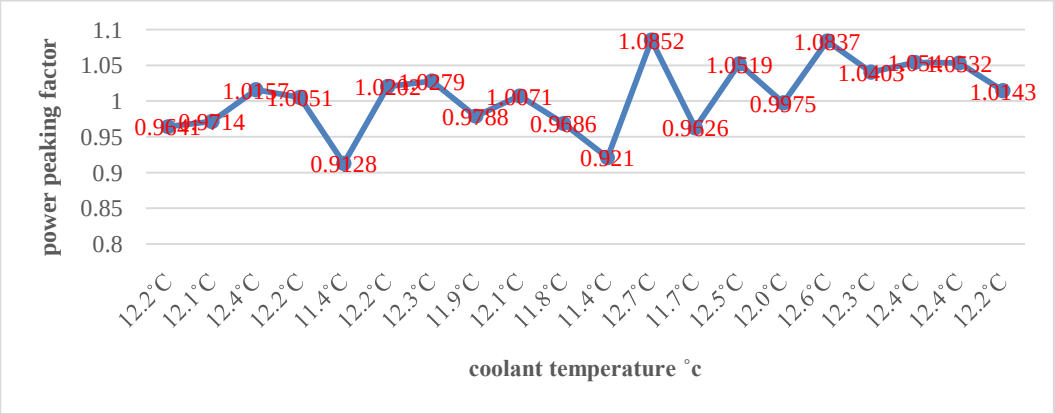


Fig: 4.4: Reactor Power Peaking Factor obtained using measured coolant temperature rise for 6hrs

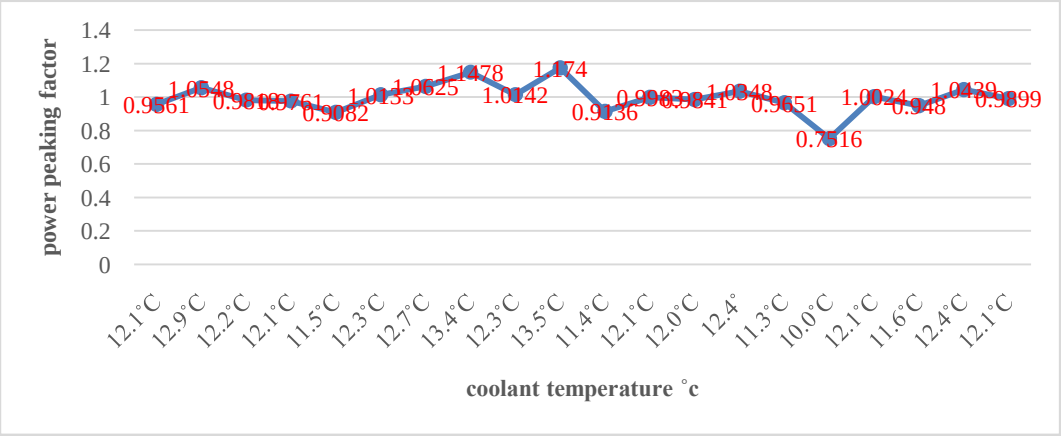


Fig:4.5: Reactor Power Peaking Factor obtained using measured coolant temperature rise for 6hrs

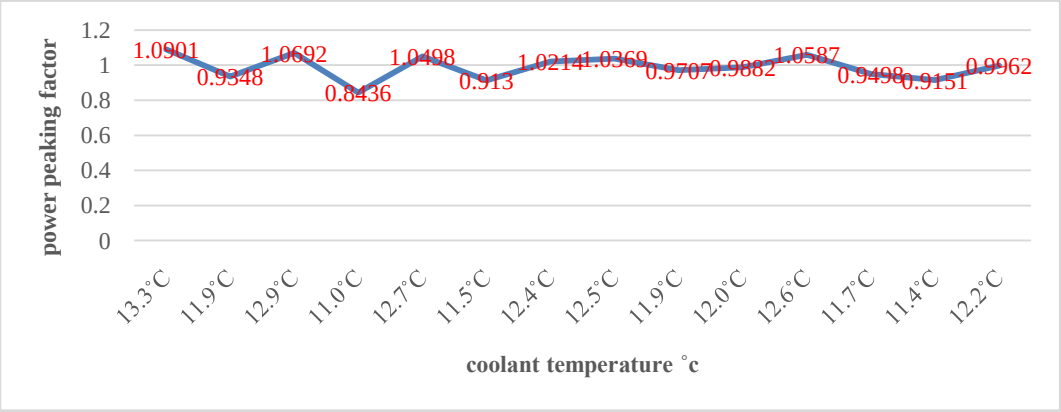


Fig: 4.6: Reactor Power Peaking Factor obtained using measured coolant temperature rise for 6hr

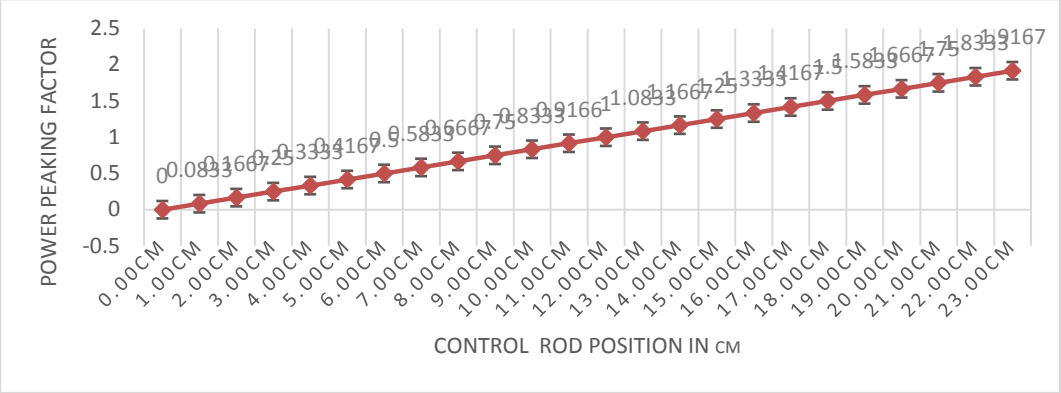


Fig. 4.7. Reactor Power Peaking Factor obtained using different control rod position in cm

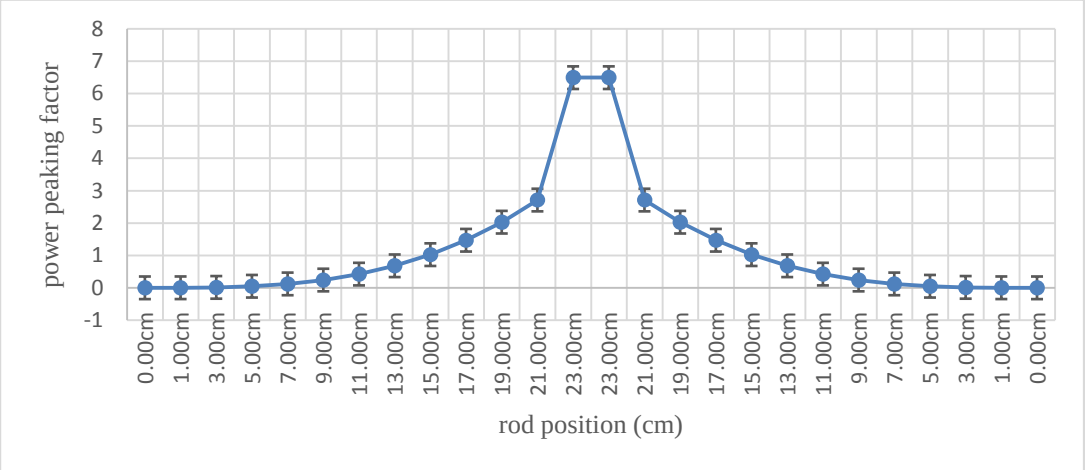


Fig. 4.8: Reactor Power Peaking Factor obtained using measured control rod position for full withdrawal

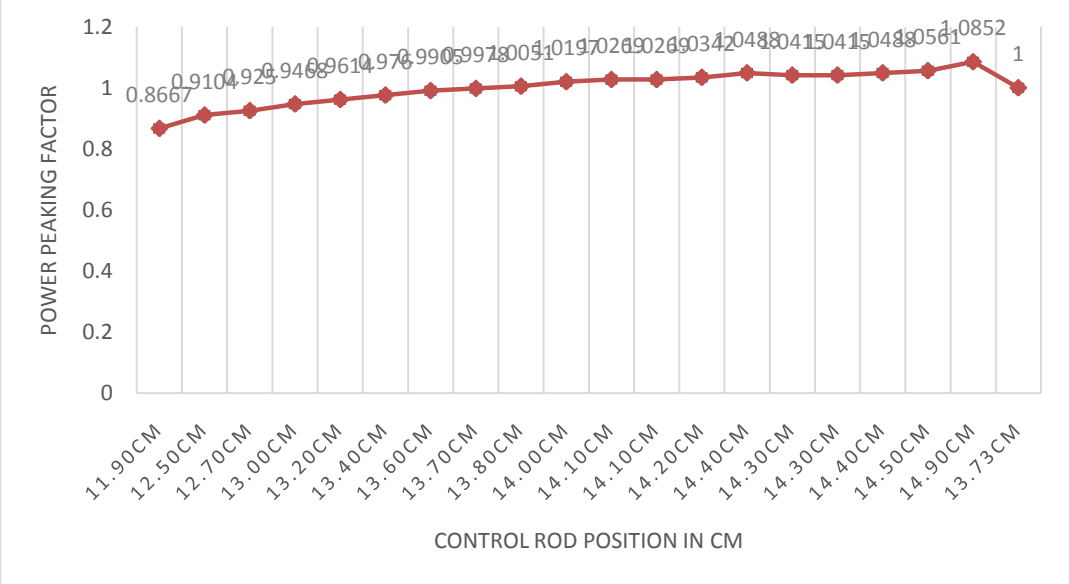


Fig. 4.9 Reactor Power Peaking Factor obtained using measured control rod position for 6hrs

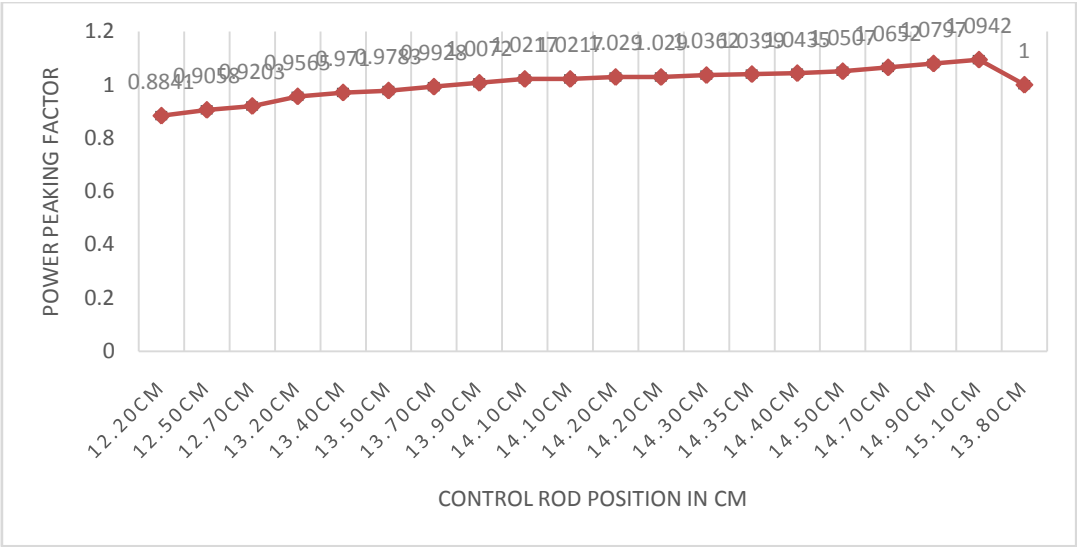


Fig. 4.10: Reactor Power Peaking Factor obtained using measured control rod position for 6hrs

4.2 Discussions

The results obtained in this work are hereby presented in table 4.1 to 4.6 below. All measurement were done at a preset flux values of 5×10^{11} n cm^2 s^{-1} and preset power of 15kW in order to study the contribution of temperature coefficient of reactivity on the reactor power stability. Just before the commencement of the experimental work and the process of reactor start up, it were observed that the inlet and the outlet temperature were all at room temperatures (24.2˚C and 24.5 ˚C respectively). These values indicate complete cooling of the reactor during the long shutdown period that preceded this work. At this start-up state, the corresponding power peaking factor was found to be 0.0027, a very low value as predicted by (In Ho Bae *et al.,* 2009, Vladimir *et al.,* (2011) and Yashar *et al*., (2012)). However a few minute after the startup of the reactor, the outlet temperature picks up rapidly to an average of 37.1 ˚C and yielding a temperature different of 13.0 ˚C. These temperature values gave rise to a sharp increase in power peaking factor due to the inherent features of the reactor and according to the rule governing insertion of excess reactivity into the reactor by the withdrawal of the control rod during the startup. (Ahmed, *et al., 2008*; 2011)

The inlet and outlet temperature values started to increase with increase in control rod withdrawal and the Power Peaking Factor oscillates around 1.00 (Table 1). These readings were collected for only 1hr after a long period of non operation. This is an indication that there is no difference between average power and preset power values. This trend continues until when the reactor begins to shut-down after about an hour of operation. Even though the inlet and outlet temperature remain steady while the reactor is being shutdown, the power peaking factor drastically reduced from 1.03 to 0.19, responding to withdrawal of excess reactively by the control rod. This is also in agreement with the fact that the average power is gradually being reduced by the

control rod while the preset flux remains constant. Figure 1 shows the two lower limits of the power peaking factor at the beginning and end of the operation. This affected the average power peaking factor of the operation which is expected to be unity. The figure also shows the oscillation of the Power Peaking Factor around 1.00 until shutdown.

The MNSR was reported by the manufacturers and some users to be stable (Shi, 1990 Yang, 1992; Ahmed *et. al*., 2008). However, our results show that the Reactor's stability is not applicable during startup and shutdown conditions. It also shows that utilization of the Reactor must wait some few minutes after startup to achieve stability and must stop some few minute before shutdown. The results also indicate the need to obtain a correction factor for sample that will stay in the Reactor for cyclic activation or for longer period of irradiation provided the Reactor will be shutdown or started in-between the irradiations. Generally Table 1 shows that allowing the reactor at a shutdown state for a longer period of time will affect its stability on start-up. It is therefore recommended that every week a test run need to be conducted even if there are no samples to be irradiated. This fact was also buttressed and supported by the result obtained in Table 4.2.

The readings in Table 4.2 were recorded for 6hrs at a different date with that of Table 4.1. It was observed that the inlet temperatures as well as the outlet temperature were all above the values of 25.0˚C and 37.6˚C respectively. This is in recognition of the fact that the reactor was operated not quite long (to obtain the readings in Table 4.1) and coolant not completely cooled during the few days period of the shutdown. These values gave an average outlet temperature of 37.6˚C and a temperature difference of 12.6˚C. These temperature values gave rise to a sharp increase in power peaking factor due to the inherent features of the reactor and according to the rules governing insertion of excess reactivity into the reactor by the withdrawal of the control rod during the

startup. As the inlet and outlet temperature values increase with increase in control rod withdrawal the Power Peaking Factor oscillates around 1.00 indicating that there was not rise in the different between average power and preset values. Figures 4.2 to 4.6 shows that the two lower limit observed in figure 4.1 was not the same because the reactor was not completely cooled during the small period of non operation and that have no significant effect on average power peaking factor of the operation and also shows the oscillation of the power peaking factor was around 1.00 at shutdown.

The result obtained here shows that there is a fairly constant reactor power (15 kW) throughout the experimental work. The thermal limitation (temperature difference) recorded during the operation has also been steady at approximately 12.6˚C. As can be seen in Tables 4.1 to 4.6 there is a steady rise in the inlet and outlet temperature with time giving approximately an average value of 31.4˚C and 42.9˚C respectively. This is due to the compact nature of the core, which was designed to cause insufficient circulation of coolant in the core. (Ahmed, *et al., 2008*; 2011) The results also revealed that NIRR – 1 could be operated at half power (flux of 5×10^{11} n cm^2 s^{-1}) for about eight continuous hours (8hrs) before the control rod attain its maximum value of 232 mm which by implication will trigger the reactor to automatically shut down. This is in agreement with the findings of Ahmed, *et al.,* (2011). This, in combination with the limited MNSR excess reactivity that is less than 0.5$ is another safety feature guaranteed by in-build negative temperature coefficient of reactivity, (Ahmed, *et al.* 2011) just in case the reactor is left unattended to for so long.

CHAPTER FIVE

(Conclusion And Recommendation)

5.1 CONCLUSION

In this work, measurements were performed to estimate the power peaking factor and thermal limitation in the Nigeria Research Reactor–1 core (NIRR-1), which is miniature neutron source reactor (MNSR). Our results show that the Power Peaking Factor for a preset neutron flux of 5.0×10^{11} $cm^{-2}s^{-1}$ ranges from 0.7072±0.2928 to 1.0143±0.0140. The average values of temperature difference recorded for all the experiments conducted were found to be constant with time and approximately equal to 12.6˚C for the whole period of operation. This is an in-build feature of NIRR-1 that compensates for high negative temperature coefficient of reactivity in order to keep the reactor at its preset power level. The average Power Peaking Factor obtained is approximately 0.9982±0.0018. This shows that, the flux in the core of NIRR-1 is stable. This is in agreement with safety requirement of the reactor which does not permit power excursion and occurrence of boiling. The outcome of the above investigation is important in avoidance of power excursion and radiation exposure to personnel and the environment despite the fact that the experimental method could not determine the exact value of power peaking factor. Therefore we are hereby recommending that further work should be carried out using simulation method to determine the power peaking factor of Nigeria Research Reactor-1 due it sealed core nature even though the computer program developed in this work can serve as a new source code for microcomputer control of the reactor peak power, maximum power factor and flux distribution at a specific time. It will also make it possible for the

microcomputer console to display real time peak power level, maximum power factor and thermal limitation of the reactor core, a tool that is lacking in MNSR design.

5.2 RECOMMENDATION.

We are hereby recommending that further work should be carried out using simulation method to determine the power peaking factor of NIRR-1 because practical estimation yielded an average value of more than 20% lower than the expected value. The computer program should be integrated into the computer control system of the Reactor, which it will enable the microcomputer console to display real time peak power level and thermal limitations of the Reactor at a given time and that there is a need to obtain a correction factor for sample that will stay in the Reactor for cyclic activation or for longer period of irradiation provided the reactor will be shutdown or started in-between irradiations.

REFERENCES

Ahmed, Y.A., Ewa, I.O.B., Umar, I.M., 2002. Effective resonance energy and non ideality of epithermal neutron flux distribution in neutron activation analysis. Nigerian Journal of Physics 14 (1), 82–85.

Ahmed, Y. A., 2004. M.Sc. Thesis: Characterization of Irradiation Channels of the GHARR-1 Miniature Neutron Source Reactor, Physics Department, Ahmadu Bello
University, Zaria, Nigeria (2004).

Ahmed, Y.A., Ewa, I.O.B., Umar, I.M., 2006. Variations in nuclear data and its impact On INAA. Journal of Applied Sciences 6 (8), 1692–1697 (Asian Network for Scientific Information, ISSN 1812-5654).

Ahmed, Y.A., Balogun, G.I., Jonah, S.A., Funtua, I.I., 2008. The behavior of reactor power and flux resulting from changes in core-coolant temperature for a miniature neutron source reactor. Annals of Nuclear Energy 35, 2417–2419.

Ahmed, Y.A., Landsberger, S., O'Kelly, D.J., Braisted, J., Gabdo, H., Ewa, I.O.B., Funtua, I.I., Umar, I.M., 2010. Compton suppression method and epithermal NAA in the determination of nutrients and heavy metals in Nigerian food and beverages. Applied Radiation and Isotopes 68, 1909 1914.

Ahmed, Y.A., Mansir, I.B., Yusuf, I., Balogun, G.I., Jonah, S.A., 2011. Effects of core excess reactivity and coolant average temperature on maximum operable time of NIRR-1 miniature neutron source reactor. Nuclear Engineering and Design 241, 1559–1564.

Ahmed, Y.A. I.B. Mansir, B.B.M. Dewu., 2013. Installation of permanent

cadmium-lined channel as a means for increasing epithermal NAA capabilities of miniature neutron source reactors. Nuclear Engineering and Design 263 (2013) 70– 76

Balogun, G. I.: Annals of Nuclear Energy, 30 (2003) 81-92

Basic Nuclear science atomiccarchive.com

Fick's laws of diffusion: http://en.wikipedia.org/wiki/Fick%27s_laws_of_diffusion

Guo, Z., 1983. Physical calculations for commercial MNSR. CIAE Technical Report.

Hainoun, A., Alisa, S., 2005. Full-scale modeling of the MNSR reactor to simulate normal operation, transients and reactivity insertion accidents under natural circulation conditions using the thermal hydraulic code ATHLET. Nuclear Engineering and Design 235, 33–52.

IAEA-TECDOC-643, ISSN 1011-4289, IAEA, Vienna. International Atomic Energy *IAEA-TEC DOC 643*: Practical aspect of operating a neutron activation analysis laboratory, IAEA, Vienna (1992)

In Ho Bae, Man Gyun Na, Yoon Joon Lee And Goon Cherl Park (2009) "Estimation of the power peaking factor in a nuclear reactor using support vector machines and uncertainty analysis" nuclear engineering and technology, vol.41 no.9

Jonah, S.A., Balogun, G.I., Umar, I.M., Mayaki, M.C., 2005. Neutron spectrum parameters in irradiation channel of the Nigerian research reactor-1 (NIRR -1) for the k0-NAA standardization. Journal of Radioanalytical and Nuclear Chemistry 226 (1), 83–88.

Jonah, S.A., Umar, I.M., Oladipo, M.O.A., Balogun, G.I., Adeyemu, D.J., 2006. Standardization of NIRR-1 irradiation and counting facilities for

instrumental neutron activation analysis. Applied Radiation and Isotopes 64, 818–822.

Jonah, S.A., Liaw, J.R., Matos, J.E., 2007. Monte Carlo simulation of core physics parameters of the Nigeria research reactor-1 (NIRR-1). Annals of Nuclear Energy 34, 953–957.

K. Fischer, T. Schulenberg, E. Laurien 2009 "Design of a supercritical water-cooled reactor with a three-pass core arrangement" Nuclear Engineering and Design 239

800-812

Khamis, I., Alhalabi, W., 2007. Assessment of cooling effects on extending the maximum operating time for the Syrian miniature neutron source reactor. Progress in Nuclear Energy 49 (3), 253–261.

M. Ravnik, 1990. Nuclear safety parameters of mixed TRIGA cores Proceedings of the Workshop on Reactor Physics Calculations for Applications in Nuclear Technology, Trieste, February 12–March 13, 1990 (1990), pp. 398–421

Mohammad Rahgoshay, OmidNoori-Kalkhoran,2013, Calculation of control rod worth and temperature reactivity coefficient of fuel and coolant with burn up changes for VVRS MWth nuclear reactor" nuclear engineering and design, volume 256, march 2013 page 322-331

Module 10 "X. Neutron and Power Distribution – Asian nuclear safety" ansn.bapeten.go.id/file/module 10 pdf

Nuclear fission Wikipedia the free encyclopedia and fission process yahoo image

Qasid Abdel Sattar, 2008, "Effect of reflector material on neutron calculation of MEU research reactor" Journal of Al-Nahrain University, Vol.11 (2), August, 2008, pp.99-10

Rahul Kharay, Nitin Bhardwaj, R. S. Jha 2009 “development of heat transfer coefficient for concentric helical coil heat exchange” International Journal of thermal Science volume 48 pp 2300-2308

R. Kapsimalis ,S.Landsberger , Y.A.Ahmed, 2009., The determination of uranium in food samples by Compton suppression epithermal neutron activation analysis. Applied Radiation and Isotopes 67 (2009) 2097–2099.

R. Khan, S. Karimzadeh, H. Boeck 2009 “TRIGA Fuel Burn-up Calculations Supported by Gamma Scanning” RRFM 2009, Vienna, Austria (2009)

R.L. Njinga, I.O.W. Ewa, S.A. Jonah, A. Baba, Y.A. Ahmed, J. Ebobenow, R. Nasiru. (2011)”Alternative Approach for Efficiency Data Generation in Neutron Activation Analysis” International Journal of Applied Science and Technology Vol. 1 No. 5;

SAR, (2005). Final Safety Analysis Report of Nigeria Research Reactor-1. CERT Technical Report-CERT/NIRR-1/FSAR-01

Shi, S., 1990. Low Power Research Reactor Thermal Hydraulics; IAEA Workshop on Low Power Research Reactors. CIAE, Beijing.

Shima Tayefi, Ali Pazirandeh 2013 “Evaluation of applying axial variation of enrichment distribution method and radial variation of enrichment distribution in VVER/1000 reactor using a Hopfield neural network to optimize fuel management” progress in nuclear energy, april, 2013 page 47 -53

Vladimir Sobes, Benoit Forget, Andrew Kadak 2011 “Individual pebble temperature peaking factor due to local pebble arrangement in a pebble bed reactor core” nuclear engineering and design, volume 241, January 2011, page 124-133.

Y. Musa, Y.A. Ahmed, Y.A. Yamusa, I.O.B. Ewa, 2011. Determination of radial and axial neutron flux distribution in irradiation channel of NIRR-1 using foil activation technique, Annals of Nuclear Energy 50 (2012) 50–55.

Yang, Y.W.: MNSR Reactor Complex Manual, CIAE, Beijing, China (1992).

Yang, Y., 1992. Reactor complex manual. CIAE Technical Report, Code MNSR DC-3.

Yashar Rahmani, Ali Pazirandeh, Mohammad B. Ghofrani, Mostafa Sadighi. Calculation of the deterministic optimum loading pattern of the BUSHEHR VVER-1000 reactor using the weighting factor method. Annals of Nuclear Energy 46 (2012) 170-181

Zhang, Y., 1984. Simulated heat transfer test for MNSR, CIAE Technical Report.

Zhu, G., 1990. Neutron Physics Experiments on Low Power Research Reactor, IAEA Workshop on Low Power Research reactors. CIAE, Beijing.

APPENDIX A

(Computer Program developed to determine power peaking factor and thermal limitation of NIRR-1 core performance)

1) **Temperature different method**

```
double p;
double t;
doubleti;
final double Pv=15.0;

    String t1=JOptionPane.showInputDialog("Enter value for coolant Temperature");
    String t2=JOptionPane.showInputDialog("Enter value for inlet Temperature");
    t=Double.parseDouble(t1);
ti=Double.parseDouble(t2);
    p=pow(E,(log(t/(7.04*pow(ti,-0.35)))*pow((0.59+0.0019*ti),(-1))));
double c=p/Pv;
JOptionPane.showMessageDialog(null,"The predicted power is"+p);
JOptionPane.showMessageDialog(null,"The power peaking factor is"+c);
```

2) **Control movement method.**

```
double p;
double h;
double r;
final double Pv=15.0;

    String t1=JOptionPane.showInputDialog("Enter value for height of reactor core");
    String t2=JOptionPane.showInputDialog("Enter value for radius of reactor core");
```

```
        h=Double.parseDouble(t1);
        r=Double.parseDouble(t2);
        p=0.004934757143*pow(r,2)*h;
double c=p/Pv;
JOptionPane.showMessageDialog(null,"The predicted power is"+p);
JOptionPane.showMessageDialog(null,"The power peaking factor is"+c);
```